AN ABSTRACT OF THE THESIS OF

John George Skinner for the Master of Science in Physics

Date thesis is presented ___April 25, 1958.___

Title ___THE PHOTOELECTRIC CURRENT FROM THE LIGHT EMERGENT___

___SIDE OF THIN SILVER FILMS AS A FUNCTION OF THICKNESS___

Abstract approved ....████████████...........

(Major Professor)

This investigation is a study of how the magnitude
and energy distribution of the photoelectric current from
the light emergent side of thin silver films varies with
film thickness. The Fowler-Dubridge graphical analysis
of the energy distribution of photoelectrons is used to
determine the energy of the most energetic of the emitted
photoelectrons, at 0°K.

The experimental phototube is of the concentric
sphere type. The silver film was deposited on the inside
of the sphere to act as a collector for the photoelectrons.
The tube was mounted on a vacuum system consisting of a
mechanical pump, an oil diffusion pump and an oil vapour
trap. During the investigation the tube was left on the
pumps at a pressure of approximately 2×10^{-7} mm. Hg. The
photocurrent from the silver film was amplified with a
Brown and Dubridge circuit using a FP-54 electrometer
tube. The film was irradiated by light from a mercury arc
lamp and a Bausch and Lomb monochromator. The intensity
of light transmitted through the silver film was monitored
by an R.C.A. IP28 electron multiplier phototube.

In order to determine the thickness of the silver
film a separate experiment was carried out to determine
the per cent light transmission through a film of known
thickness. The main investigation consisted of depositing
a layer of silver on the quartz disc mounted in the center
of the experimental tube, and measuring the percentage of
transmitted light, of wavelength 2483A, through the film.
The emitted photocurrent was then measured as a function
of the light intensity at the light emergent side of the
silver film, and as a function of the retarding potential
across the experimental phototube. The film was increased
in nineteen steps to a maximum thickness of 255A, and the
above data was recorded for each film thickness.

The magnitude of the photocurrent increased with film thickness up to about 40A and was then relatively constant for thicker films. The analysis of the energy distribution of the photocurrent showed an increase of the maximum energy of emission with film thickness up to about 50A. This increase in maximum energy may be due to a change in contact potential between the collector and the silver film or to a decrease in the work function of the silver film as the thickness increases. A decrease in the work function of the silver film, with increasing thickness, would explain the increase in the emitted photocurrent, with increasing film thickness.

THE PHOTOELECTRIC CURRENT FROM THE LIGHT
EMERGENT SIDE OF THIN SILVER FILMS
AS A FUNCTION OF THICKNESS

by

JOHN GEORGE SKINNER

A THESIS

submitted to

OREGON STATE COLLEGE

in partial fulfillment of
the requirements for the
degree of

MASTER OF SCIENCE

June 1958

APPROVED:

_____
Professor of Physics

        In Charge of Major

_____
Chairman of Department of Physics

_____
Chairman of School Graduate Committee

_____
Dean of Graduate School

Date thesis is presented April 25, 1958.

Typed by Elizabeth Skinner

ACKNOWLEDGEMENT

TABLE OF CONTENTS

TABLE OF FIGURES

TABLE OF PLATES

THE PHOTOELECTRIC CURRENT FROM THE LIGHT EMERGENT SIDE OF THIN SILVER FILMS AS A FUNCTION OF THICKNESS

INTRODUCTION

General. If a study is made of the work done by previous experimenters in the field of photoelectric emission from the thin metal films it becomes evident that there is a wide discrepancy in the data that has been published. The results are generally tabulated by plotting the photocurrent, at a constant light intensity and wavelength, against film thickness.

Werner (9, p.494), who investigated gold films sputtered on glass, found that the photocurrent increased with film thickness up to 300A then remained relatively constant, see Figure 1a. Rubens and Ladenburg (9, p. 494) found that the maximum current occurred at a film thickness of 1000A. Stuhlmann (14) investigated films of silver and platinum evaporated on quartz and found that the photoelectric emission at first increases with the thickness, then diminishes as the thickness is increased, and finally begins to increase again with thickness, see Figure 1b. Compton and Ross (2) studied sputtered films of platinum and gold. A typical set of curves for different wavelengths is shown in Figure 1c. Dember and Goldschmidt (9, p. 496) repeated the work of Compton and Ross with the results
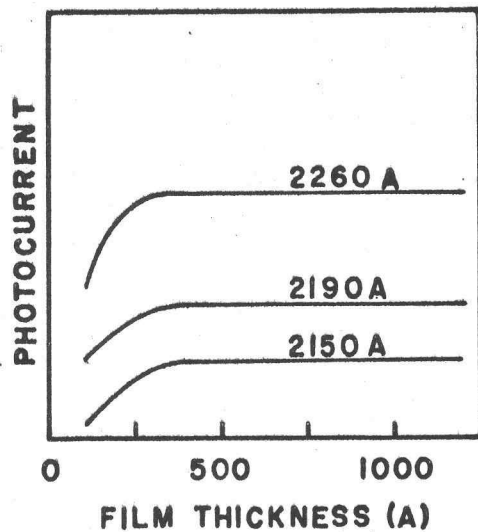
FIG. IA – GOLD SPUTTERED ON GLASS.
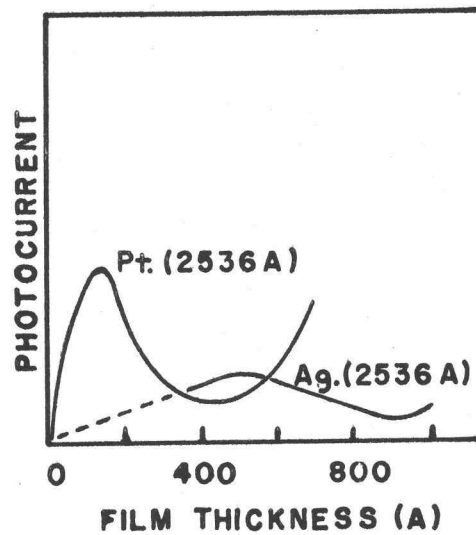
FIG. IB – PLATINUM AND SILVER EVAPORATED ON QUARTZ
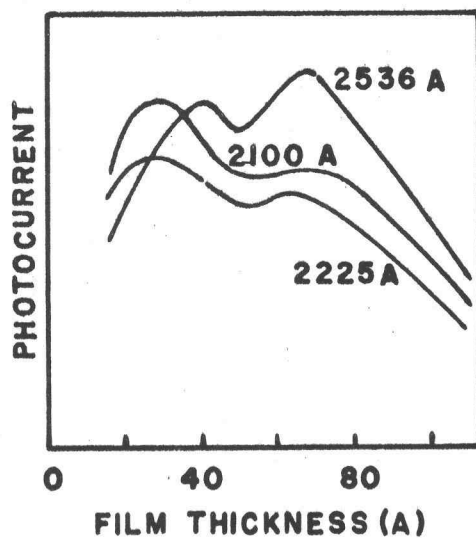
FIG. IC – PLATINUM SPUTTERED ON GLASS.
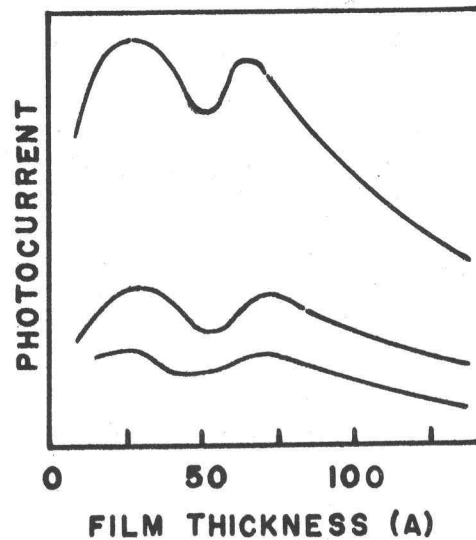
FIG. ID – SPUTTERED PLATINUM FILMS.

FIGURE I. RESULTS OF PREVIOUS WORKERS.

PHOTOCURRENT AS A FUNCTION OF FILM THICKNESS.

THEORY

The photoelectric effect has been described as "one in which the absorption of radiation by matter produces an electrical change". In this investigation we are concerned with some aspects of the release of electrons from a metal surface by the action of radiation.

Since the discovery of the photoelectric effect by Hertz in 1887 it has been the subject of much investigation (4, 9). In 1905, Einstein applied the quantum theory to the phenomenon and was led to his famous equation:

$$mv_m^2/2 = h\nu - h\nu_o$$

where v_m = maximum velocity of emitted electron

   ν = frequency of incident radiation

   ν_o = threshold frequency of the surface

This was verified by various workers who showed that there was a sharply defined maximum velocity v_m as given by the equation. Later, workers with more sensitive equipment found that there was no well defined maximum velocity and that the number of electrons, whose velocity was greater than v_m, decreased asymptotically to zero; this could not be explained.

The basis for the new electron theory of metals was laid in 1928 by Sommerfeld who applied Fermi-Dirac statistics to the distribution of kinetic energy among the "free" electrons in the metal. Both the old and new theories

assume that in any conductor there are large numbers of free electrons capable of wandering about in the spaces between the atoms. The interior of the metal is assumed to be a region of constant potential with a potential-barrier at the surface to keep the electrons in the metal. In the classical theory (old) it is assumed that these electrons have the same mean kinetic energy of thermal agitation as the atoms, namely $(3/2)kT$, with the energies of individual electrons being distributed about this mean according to the Maxwell distribution function. The Sommerfeld theory (new) discards the equipartition theorem and treats the electrons as a degenerate gas obeying the Fermi-Dirac statistics. Whereas at 0^OK, the old theory regards the electrons at rest, the new theory shows they have energies up to the order of 10 electron volts. Calling this maximum energy μ_m, it is evident that the threshold frequency at 0^OK is given by:

$$h\nu_o = W_a - \mu_m = \emptyset e$$

where W_a = surface potential barrier

$\emptyset e$ = work function of surface.

The theory shows that Einstein's equation is only accurately true at 0^OK while at higher temperatures there will not be a sharply defined maximum velocity. The theory goes further by predicting the form of the energy distribution and spectral distribution curves at any temperature.

The most useful theory of spectral distribution was developed in 1931 by R. H. Fowler (7). Although the spectral distribution is not considered in this analysis, the logical steps of Fowler's theory make an ideal introduction to the analysis of the energy distribution. The general procedure for deriving an expression for spectral distribution would consist ideally of the following steps:

1. Set up the velocity distribution function $f(u)du$ for electrons in metal. This is the Fermi-Dirac function for the number of electrons per unit volume having velocity u, independent of direction, in the range du and is given by:

$$f(u)du = \frac{8\pi\, m^3}{h^3}\left[\frac{1}{e^{(\mu-\mu_m)/kT}+1}\right] u^2 du$$

where $\mu = \frac{mu^2}{2} = \frac{m}{2}\left[u_x^2 + u_y^2 + u_z^2\right]$

$$\mu_m = \text{constant} = \frac{h^2}{2m}\left[\frac{3n}{8\pi}\right]2/3$$

n = total number of electrons per unit volume.

2. Compute the probability P that an electron with velocity u will absorb a quantum $h\nu$. The product $P \cdot f(u)$ will be the number of excited electrons with energy:

$E_1 = mu_1^2/2 = mu^2/2 + h\nu$

3. Derive the distribution function $f(u_n)$ for the excited electrons in terms of the component of velocity perpendicular to the surface, i.e. normal component u_n.

4. Multiply $f(u_n)$ by the transmission coefficient D for the surface potential, this is simply the fraction of electrons with velocity u_n which will penetrate the surface potential barrier W_a.

5. Integrate over all values of u_n to get the number of electrons escaping per second.

Fowler built his theory around the fact that in experimental work on ordinary metals the highest frequency in the ultraviolet that is usually available to the experimentalist does not exceed the threshold frequency by more than 50 per cent. Therefore, the experimentalist is primarily interested in a theory that is reasonably accurate in the vicinity of the threshold frequency. With this limitation the electrons which can be ejected from the metal are those whose initial energies lie within a few per cent of the maximum energy allowed by the Fermi-Dirac statistics. Since these are the electrons which are most affected by temperature changes then the temperature must be considered in the calculations.

With this frequency limitation, then since the

initial velocities of electrons which are ejected lie in a relatively small range, any probability factors which depend on a small power of this velocity may be considered constant. Thus we may assume that the probability P is constant so that steps 1 and 3 may be combined. We may further assume that the transmission coefficient D is zero for electrons whose "normal energy" E_n is less than W_a and is unity for those whose " normal energy " E_n is greater than W_a. The "normal energy" is the kinetic energy associated with the velocity component normal to the surface, $E_n = mu_n^2/2 = $ initial "normal energy" plus $h\nu$. The procedure for deriving the spectral distribution is now reduced to two steps:

1. Set up the function expressing the number of electrons striking unit surface area per second with "normal energy" E_n in the range dE_n.
2. Integrate over all value of E_n greater than the critical value given by $E_{no} + h\nu = W_a$.

The result gives the number of electrons N per second coming up to a unit area of surface from within, with normal energies sufficient to escape,

where $N = (4 \pi m k^2 T^2 / h^3) \Theta(x_o)$

$\Theta(x_o) = $ complicated function of x_o

$$x_o = \frac{h\nu - h\nu_o}{kT}$$

We may assume that the photocurrent I is proportional to eN:

$$I = \alpha \, eN$$

where e is the electron charge

α is the proportionality factor.

The final equation for the spectral distribution may be written in the form:

$$I = \alpha \, A \, T^2 \, \theta(x_0)$$

where A is a universal constant $= 4 \pi m e k^2/h^3$

The methods used in developing Fowler's theory of spectral distribution were extended by Dubridge (3) to the problem of the energy distribution of photoelectrons. Experimentally the energy distribution is usually determined by noting the photoelectric current reaching a collector electrode as a function of the retarding potential V applied between this electrode and the emitting surface. The form of the resulting current-voltage curve will depend on the geometrical arrangement of the two electrodes. If the electrodes are parallel plates then the distribution of the "normal energy" is obtained, if the electrodes are concentric spheres the total-energy distribution is obtained. We shall consider the total-energy distribution.

The general procedure follows a similar line to that for the spectral distribution:

1. Set up the velocity distribution function $f(u)du$.

2. Compute the probability P that an electron with velocity u will absorb a quantum $h\nu$.

3. Of the excited electrons only those can escape whose velocity u_1 is so directed that its component u_n normal to the surface is greater than the minimum value u_{nc} required to surmount the potential barrier, so that $mu_{nc}^2/2 = W_a$. This means that the vector u_1 must lie within a cone with axis normal to the surface and whose half-angle at vertex is arc cosine (u_{nc}/u_1), and therefore subtends the solid angle $2\pi(1-u_{nc}/u_1)$. The chance of the vector lying in this cone is the ratio of this solid angle to 4π and is therefore $(1-u_{nc}/u_1)/2$ providing u_1 is greater than u_{nc} and is zero for u_1 less than u_{nc}.

   Electrons with original velocity u in the range du will, after escape, have a velocity v in the range dv where $$\frac{mv^2}{2} = \frac{mu_1^2}{2} - W_a = \frac{mu^2}{2} + h\nu - W_a$$

   If we multiply the number of electrons per unit volume having velocity u_1 by the value of the velocity component u_n normal to the surface we obtain the number arriving at unit area of surface in unit time.

4. Multiply by the transmission coefficient $D(v)$ of the surface, for electrons with velocity v. Note that the transmission coefficient $D(v)$ is the probability of an electron with sufficient energy to escape actually escaping. Although, as it is shown later, $D(v)$ is considered to be constant it need not actually be so. The number of electrons escaping from unit area in unit time with velocity v in the range dv is then given by :

$$N(v)dv = u_n \ P \ D(v) \ (1-u_{nc}/u_1)/2 \ f(u)du$$

Expressing the above equation in potential units by the relation $V^1 e = \dfrac{mv^2}{2}$ we obtain $N(V^1)dV^1$. The current I reaching the collector when the retarding potential is V is then given by

$$I = e \int^{\infty} N(V^1)dV^1$$

If the theory is restricted to the same frequency limitations as for the spectral distribution, the factors P and $D(v)$ are essentially constant.

The complete derivation of the above equation is too lengthy for this summary but it can be shown that within the limitations

$$(x-x_0) > 1 \text{ and } x_0 > 10$$

then I can be expressed as

$$I = A \ T^2 \ x \left[e^{-(x-x_0)} - \frac{e^{-2(x-x_0)}}{4} \right]$$

where $x = \dfrac{Ve}{kT}$ and $x_0 = \dfrac{V_m e}{kT} = \dfrac{h\nu - h\nu_0}{kT}$

A large part of the usefulness of Fowler's theory is the graphical method which he proposed for the analysis of experimental data. We may write the above equation for energy distribution in the form:

$$\log_{10} (I/x) = B + f(x-x_0)$$

where $B = \log_{10} (\propto A\ T^2) =$ a constant for constant temp.,

$$f(x-x_0) = \log_{10} \left[e^{-(x-x_0)} - \frac{e^{-2(x-x_0)}}{4} \right]$$

From this equation we see that $\log(I/x)$ is a universal function of $(x-x_0)$. A plot of $\log(I/x)$ against $(x-x_0)$ should be the same as $f(x-x_0)$ except for the vertical displacement equal to B. Also a plot of $\log(I/x)$ against (x) should be the same as a plot against $(x-x_0)$ except for a horizontal shift equal to x_0. Thus from a plot of $f(x-x_0)$ against $(x-x_0)$ and $\log(I/x)$ against (x), the value of x_0 and hence V_m can be determined. The numerical values for $f(x-x_0)$ are tabulated for reference in Table 4.

In this summary it has been assumed that the free electron absorbs the entire energy of the impinging quantum, and no attempt will be made to explain the combining mechanism.

It should be noted in this theory that the photo-current has been shown to be dependent on the number of electrons arriving at the surface of the emitter suggesting that the photoelectric phenomenon is a surface effect.

The Fowler theory has been tested by many workers (4, 9) and has been shown to be very accurate over the range for which it was developed.

In this investigation the above theory will be used for the following considerations:

1. The results of the photocurrent versus film thickness data will be analyzed on the assumption that the photoelectric phenomenon is a surface effect.

2. The graphical method of analysis will be used to determine if the work function of the silver film changes with film thickness.

APPARATUS

General. The complete apparatus layout is shown schematically in Figure 2; a list of the equipment is included in the appendix. Unless otherwise stated, the terms "silver film" and "emitter" refer to the thin film being investigated.

The experimental phototube is of the concentric sphere type and is shown in Figure 3. The silver film was deposited on the quartz window mounted in the center of the tube, silver was also deposited on the inside of the sphere to act as a collector for the photoelectrons. The silver was evaporated from three equi-spaced filaments, a shield was included inside the tube to prevent the silver film and collector being shorted out. A potential can be applied between the emitter and the collector.

The tube was made complete with ion gauge, oil vapour trap, and diffusion pump connection. The ion gauge is a Vecco RG75-P gauge, and the oil vapour trap a corrugated copper foil type (1). During the investigation the tube was left on the pumps at a pressure of approximately 2×10^{-7} m.m. Hg.

The photocurrent from the silver film was amplified with a Brown and Dubridge circuit using a FP-54 electrometer tube. The amplifier was used as a null balancing device, a voltage from the calibrating circuit balanced

the voltage produced across the grid resistance by the photocurrent. This method eliminates errors due to changes in amplifier gain.

The film was irradiated by light from a mercury arc lamp and a Bausch and Lomb monochromator. The wavelength of the light was 2483A. The intensity of light transmitted through the film was monitored by an R.C.A. 1P28 electron multiplier phototube, the output of which was measured on galvanometer II, see Figure 2.

The monochromator and electron multiplier phototube are mounted on a platform which is pivoted near the multiplier phototube; a journal ball bearing being used for the pivot. The purpose of the platform is to enable the monochromator and the detector to be swung clear of the experimental phototube so that the intensity of the ultra-violet light may be measured directly. This enables the per cent transmission of the light through the photo-tube to be determined which in turn can be used to deter-mine the thickness of the silver film. This is explained in more detail in the section on procedure.

Experimental Phototube. The tube was constructed from a two-litre Pyrex glass flask, with two Pyrex-to-quartz seals for the quartz windows. It was originally intended to deposit the collecting surface after the tube was mounted on its final vacuum system, this would avoid

any contamination of the surface and any change in the
work function of the collecting surface. This method re-
quired a shield that would cover the center quartz window,
while the collector surface was deposited, and could then
be removed to deposit the silver film and carry out the
investigation. The cover was mounted on a long vertical
arm which projected down from the center of the sphere,
and could be operated magnetically. The pump-out aperture
was situated approximately where the vertical projection
for the ion gauge was finally located.

Several difficulties were encountered in the con-
struction of the tube. One set of quartz windows was cut
from crystalline quartz and completely shattered while
being heated. Another set of windows was made from fused
quartz; these were used successfully. The window thickness
was 3-4m.m. Several tubes broke after construction, one
broke around the collector lead; after repair it broke
around the oil vapour trap. After rebuilding, the tube
remained intact until assembled on the vacuum system; when
the vacuum pump was turned on, the inner glass-to-quartz
seal shattered. Although the tube was annealed at various
stages in its construction the available ovens were not
large enough to anneal the complete assembly.

It was decided to eliminate the cover, for protecting
the inner quartz window, and make the tube and vapour trap
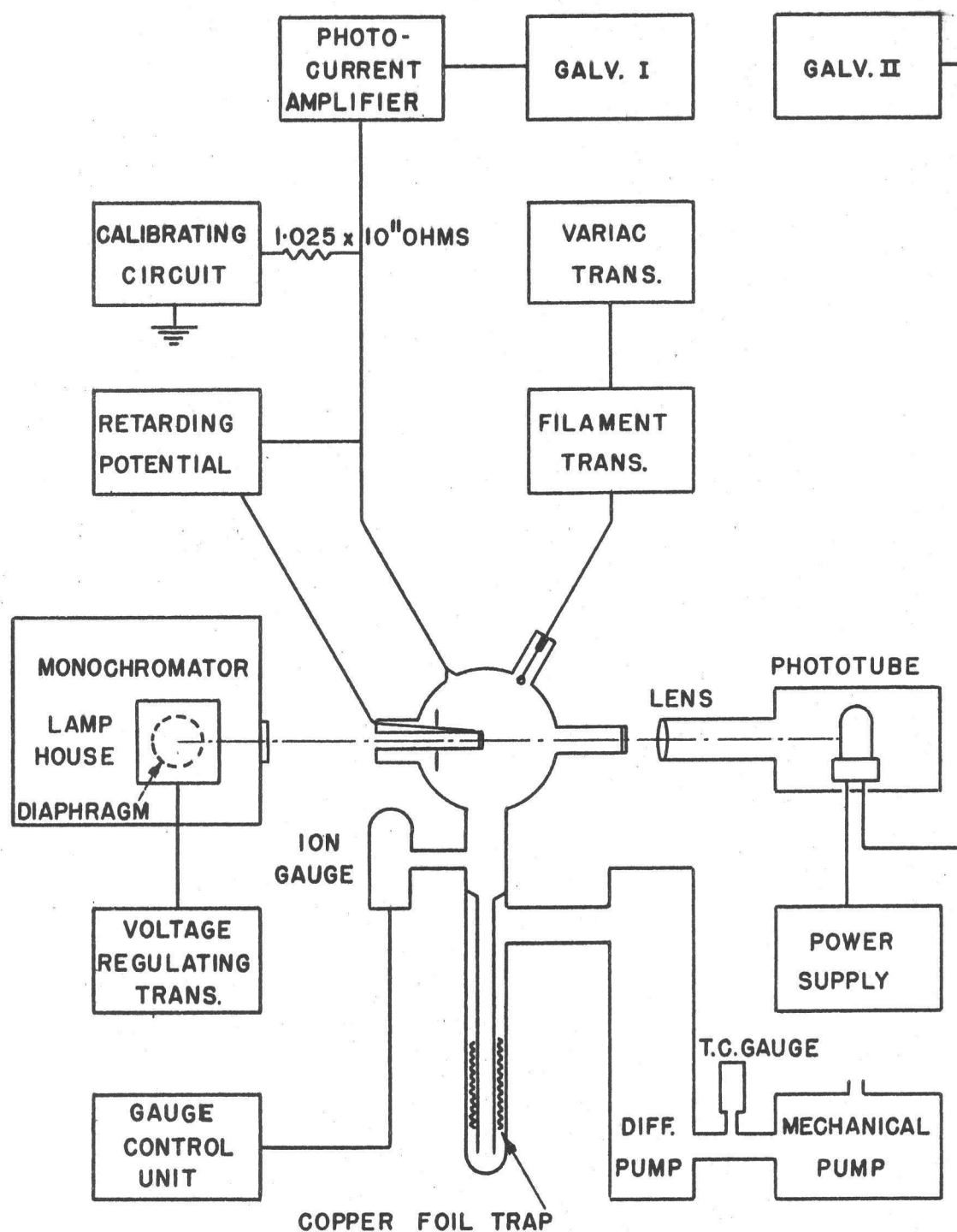
FIGURE 2.   SCHEMATIC   LAYOUT   OF   EQUIPMENT

30° 30°

3 EQUI-SPACED
CONNECTIONS TO
INSIDE OF SPHERE

3 EQUI-SPACED
FILAMENTS FOR
EVAPORATING SILVER

SILVER FILM

U.V.
LIGHT

SHIELD

TWO QUARTZ WINDOWS

30 m.m.

30 m.m.

7·5 ins.

14 ins.

45 m.m.

6·5 ins.
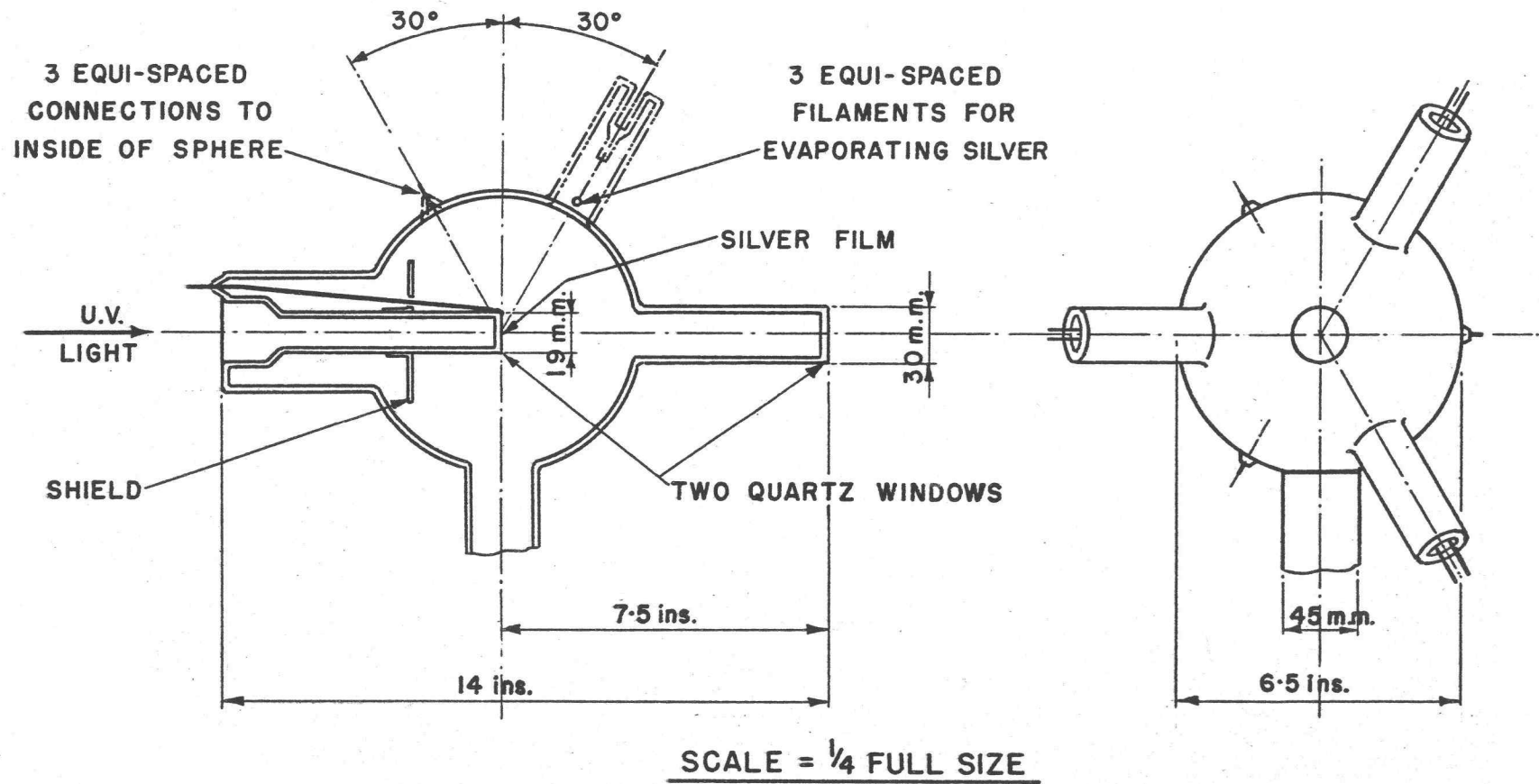
SCALE = ¼ FULL SIZE

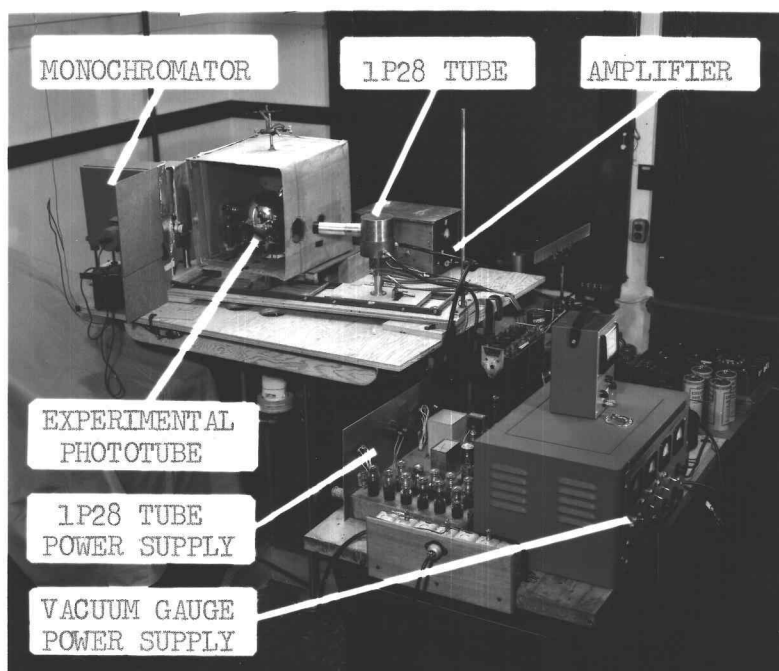FIGURE 3. EXPERIMENTAL PHOTO-TUBE

17

PLATE 1. LAYOUT OF EQUIPMENT.
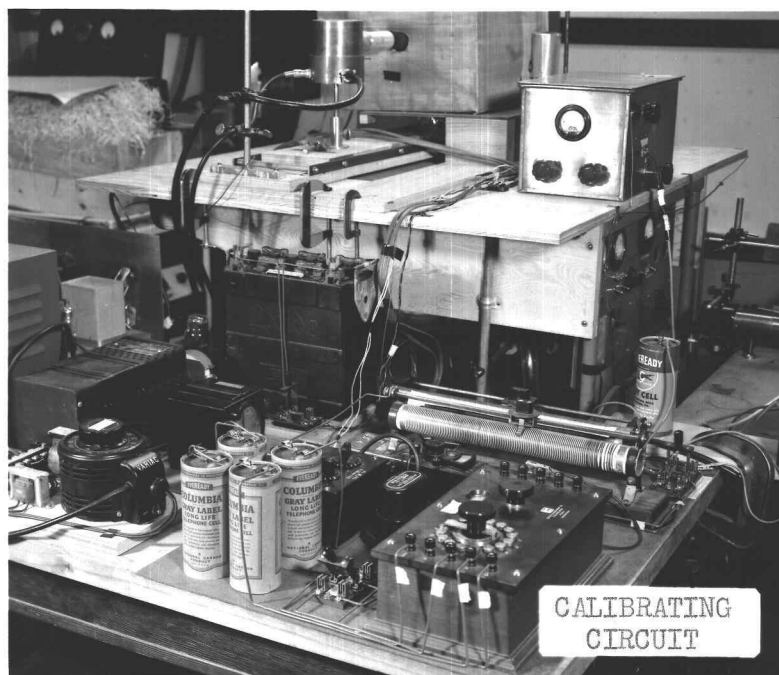
PLATE 2. LAYOUT OF EQUIPMENT.
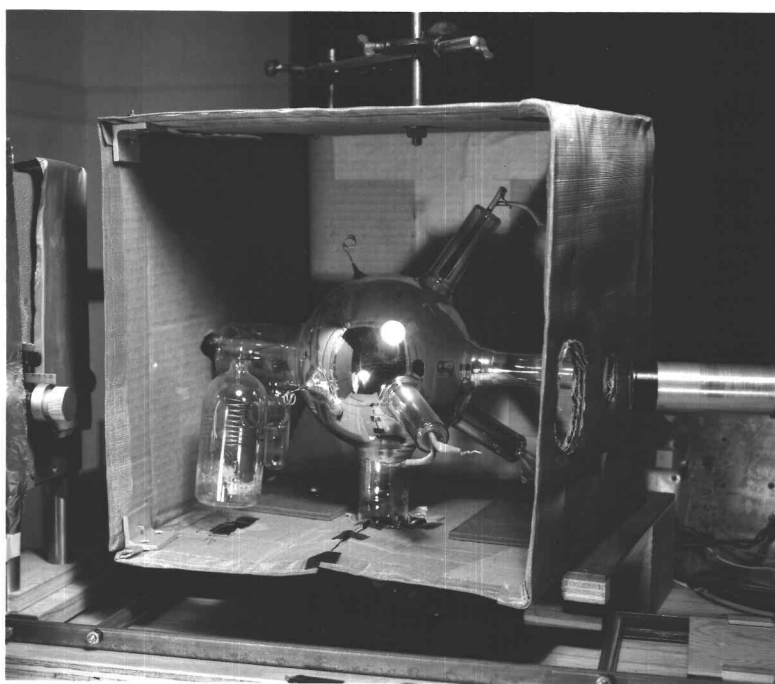
PLATE 3. EXPERIMENTAL PHOTOTUBE.
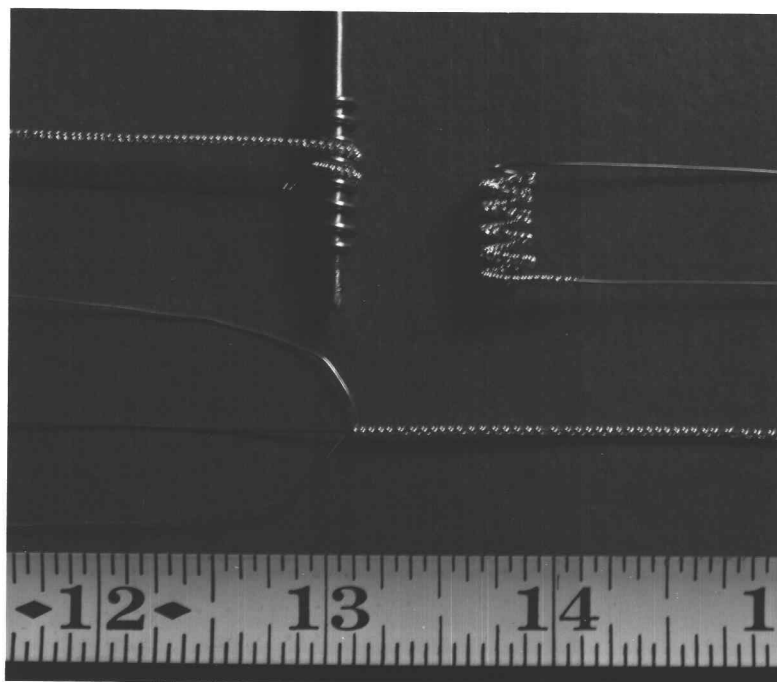
PLATE 4. FILAMENT CONSTRUCTION.

separately, anneal them, then join them together with the least amount of heating. The collecting surface was deposited inside the sphere during the construction of the tube. The three collector leads were tungsten wires in uranium glass "buttons". Inside the tube, the tungsten wires were surrounded and connected with a conducting silver paint which was painted on the surface of the glass then fired at a suitable temperature. This makes a good mechanical bonding to the glass and provides a good electrical contact between the deposited silver collector and the collector leads. Connection to the silver film on the center quartz window was made by embedding a tungsten wire into the quartz, then painting around the wire and the edge of the quartz window with the silver conducting paint.

The copper trap was made by a previous worker (12,p. 15-17), it was cleaned in a hydrogen furnace prior to assembly in the oil vapour trap.

The filaments were made by winding 20 inches of 28 gauge silver wire (99.9% pure) around 0.015 inch diameter tungsten wire, then winding the tungsten wire into a five-coil spiral approximately half inch long, (see Plate 4). The silver wire extended down the shank of the coil on one side and was left clear of one tungsten coil on the other side. Only the silver near the clear tungsten

coil became hot enough to evaporate, the rest of the coil
was "shorted" out by the silver. The filament was made in
this manner to provide a slow method of evaporation, and
low power consumption. The low power requirement was to
avoid overheating the tungsten leads which passed through
the glass. Unfortunately although the rate of evaporation
was slow it was also uneven, depending on whether the
point of evaporation was at the back or the front of the
filament. This uneven rate of evaporation produced an
extra thick silver film at one point during the investi-
gation. Various filament designs were tried prior to
deciding on the above construction. One was a four coil
filament of silver wire interlaced into a five coil tung-
sten filament. The silver coil would not stay interlaced
in the tungsten filament, but dropped to the bottom of the
tungsten coils where it eventually melted at the points of
contact and broke into separate rings. Other designs
consisted of a small bar of silver 0.3 inches x 0.05
inches x 0.05 inches enclosed in parallel or tapered wound
tungsten filament. It was found that these designs
required higher power inputs than the chosen design.

Consideration was also given to the film thicknesses
that could be obtained with the available silver on the
filaments. The "silver bar" design would give a thickness
of about 6000A. on the center quartz window and about

1000A. on the furthest side of the experimental tube.
Since the chosen design would give approximately three
times this amount this was another factor in favour of
the adopted design.

An excessive amount of silver was used to form the
collecting surface and although the extra silver was
necessary in this experiment, with careful deposition the
volume of silver in the bar design should be sufficient.
A design using a bar of silver would be better in order
to obtain even distribution.

Vacuum System. This consists of an Eimac HV-1 oil
diffusion pump, a Cenco Megavac mechanical pump and a
thermocouple gauge between the two pumps. The ultimate
vacuum of the diffusion pump is listed at 4×10^{-7}mm.Hg.
of pressure with Eimac type A oil. An attempt was made to
obtain a lower pressure by using teflon gaskets, at the
head of the pump, and Octoil-S diffusion pump oil. These
tests were carried out with the diffusion pump capped off
at the head. The teflon gasket was unsuccessful because
the diffusion pump connection, attached to the experimental
tube, had been previously ground and the O-ring groove had
been considerably reduced. This prevented the teflon gas-
kets from seating and sealing properly, so it was decided
to use rubber gaskets.

The temperature of the diffusion pump heater was

varied to obtain the best operating conditions with the
Octoil-S oil. There was little change in pressure for
changes in heater voltage from 106 to 116 volts, therefore,
110 volts was used for convenience. The lowest pressure
obtained was 6 x 10^{-7} mm.Hg., since this pressure was meas-
ured directly at the input to the diffusion pump it was
considered that the pressure would be lower when the vapour
trap was included in the system. Lowest pressure obtained
with completed system, after bakeout, was 4 x 10^{-8} mm.Hg.
The diffusion pump is mounted on a frame which also sup-
ports the monochromator, photo multiplier, and amplifier.
To avoid unnecessary vibration the diffusion pump cooling
fan, and the mechanical pump are mounted independently on
the floor. The Veeco ionization gauge was operated from
an available Radiation Laboratory type gauge power supply
and the output measured with an R.C.A. microammeter.

Oven. A portable oven was made to bake out the
experimental tube. It was made from 1/2 inch asbestos
sheet and had internal dimensions of 19-1/2 inches x 18
inches x 15-1/2 inches high. During bakeout, the oven was
covered with two asbestos blankets. The oil vapour trap
was baked out with a cylindrical oven which was already
available. Asbestos tape was wrapped around the portion
of the tube between the main oven and the cylindrical oven
to prevent a temperature gradient. The main oven had

four 1000 watt heaters and a circulating fan. Copel-chromel thermocouples were attached to the oil vapour trap, ionization gauge, extreme top of the tube, the 30mm. diameter quartz window and the top of the diffusion pump to monitor the temperature and to avoid uneven heating. The oven power was obtained through a separate main power fuse for safety. Whenever the tube was baked out, the heater voltages were increased approximately 10 volts every 10 minutes. A maximum tube temperature of approximately 400°C could be obtained.

Monochromator and Method of Calibration. The instrument used was a Bausch and Lomb Grating Monochromator, 250mm. focal length, with a dispersion of 66A per mm. at the exit slit. The calibration was done in the visible region by observing lines of known wavelengths and noting the corresponding wavelength dial reading. It was found that the instrument had an error of approximately 95A, and that the error increased towards the ultra-violet end of the spectrum. A more accurate calibration was carried out in the ultra-violet region by taking a reading every 10A, using a thermocouple as a detector, then comparing the results with a spectrum of the mercury arc lamp and the known spectrum of a mercury arc. The results are shown on Figure 4., the entrance and exit slit were 0.25mm. wide. The instrument was approximately 120A in error in the

ultra-violet region. The 2537A line is not so large, in comparison with neighboring peaks, as that shown in listed values. There is also an absorption line on the spectrum of the mercury lamp at 2537A suggesting self absorption. The 2483A line and a slit width of 0.1mm. was used in the investigation as this was found to give the best compromise between the photocurrent from the experimental tube and the output of the ultra-violet detector.

A study was made to determine how stable the ultra-violet light intensity was with changes in voltage applied to the mercury arc lamp. It was found that the intensity increased linearly by a factor of five for a change from 75 volts to 120 volts. It was decided to use a Sola 115 volt, 250 volt-ampere constant voltage transformer to avoid intensity functuation due to line voltage changes.

Optical System. This consists of one quartz lens with a focal length of 17cms. The lens is mounted on the front of the ultra-violet detector housing at a distance of 26cms. from the detector and 46cms. from the monochromator, with the experimental tube centered between the monochromator and the lens. The experimental tube is enclosed in a light tight box, except for light entrance and exit, the 19mm. glass to quartz tube was blacked out to avoid scattering of light on to the photoelectron collecting surface.

SPECTROSCOPIC PLATE OF MERCURY ARC

MERCURY ARC
SPECTRUM

IRON
SPECTRUM

2400   2600   2800   3000 A
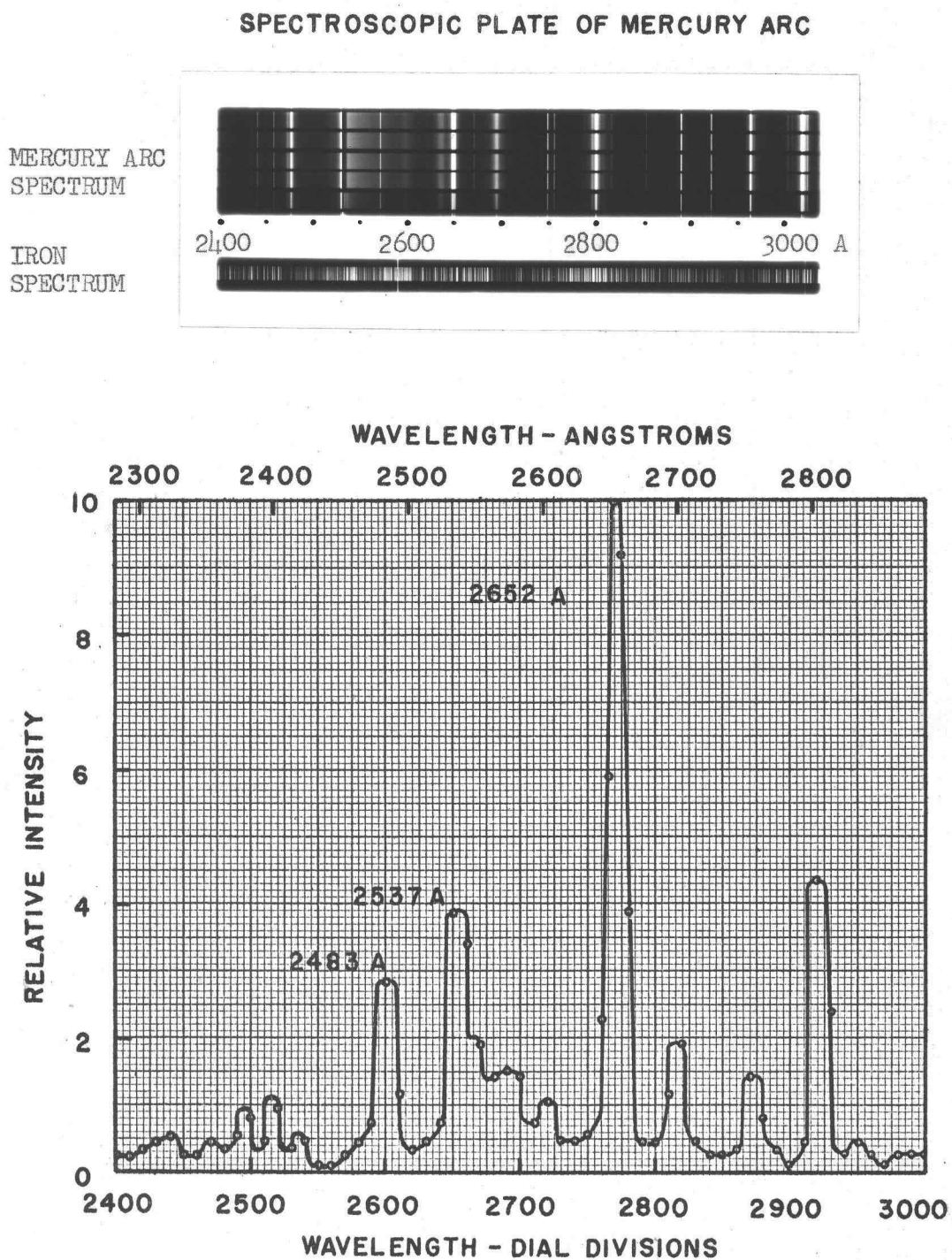

WAVELENGTH – ANGSTROMS

FIGURE 4. SPECTRUM OF MERCURY ARC LAMP

An iris diaphragm is mounted on the front of the mercury arc lamp to enable the intensity of the ultra-violet light to be varied. A shutter was placed over the front of the monochromator when it was required to shut the light off from the experimental tube.

Ultra-violet Light Detector. The original detector was a bismuth and tellurium thermocouple enclosed in an evacuated chamber and surrounded by a water jacket and glass wool, an attempt was made to use this because of its simplicity. The maximum voltage output obtained from the thermocouple, for maximum available ultra-violet light intensity, was approximately 12 micro-volts or 21 cm. galvanometer deflection, without the experimental photo-tube in the system and using a monochromator exit slit width of 1mm. By lagging the thermocouple leads to the galvanometer a stability of 0.1cm. galvanometer deflection per hour was obtained. When the experimental phototube was completed and assembled in the system the thermocouple output was only a few centimeters of galvanometer deflection due to the poor transmission through the tube. It was decided to use an electron multiplier phototube for the detector.

An R.C.A. 1P28 phototube was chosen because of its spectral range and availability, a suitable power supply and phototube housing was also available. A preliminary

test with a monochromator slit width of 1/2mm. and a wave-
length of 2483A gave a galvanometer deflection of 22,000cm.

Amplifier and Calibrating Circuit. The amplifier is
a Brown and Dubridge circuit (5) using a FP-54 electro-
meter tube and a grid resistance of 1.025×10^{11} ohms. The
output of the amplifier was measured on galvanometer I
through an Ayrton shunt, set at x10 attenuation. The
overall sensitivity was 6×10^{-15} ampere per centimeter
of galvanometer deflection, with x1 attenuation, and the
noise level was less than 10^{-14} ampere. The amplifier
current gain was 5×10^{6}; this appears to be large but
the value was checked several times. Considerable
difficulty was encountered in setting up the amplifier
but it was finally set as per directions in reference 5.

The light tight box around the experimental tube is
also an electrostatic shield. All filament and ion gauge
leads were removed from within the shield during the
investigation. Originally the experimental phototube was
bound with aluminum foil, for electrostatic shielding,
but this gave an amplifier time constant of 8 minutes
because of the relatively large electrostatic capacity.
With the large box around the tube the time constant was
approximately 30 seconds.

The calibration circuit (10, p. 8) is a basic layout
using a Leeds and Northrup Students Potentiometer; it was

BASE OF FP-54

GALV. I   AYRTON SHUNT   AMPLIFIER

FP-54

RETARDING POTENTIAL

EXPERIMENTAL PHOTO-TUBE

CALIBRATING CIRCUIT

$1.025 \times 10^{11} \Omega$

$10K\Omega$

50

$4K\Omega$

I_F

$2K\Omega$

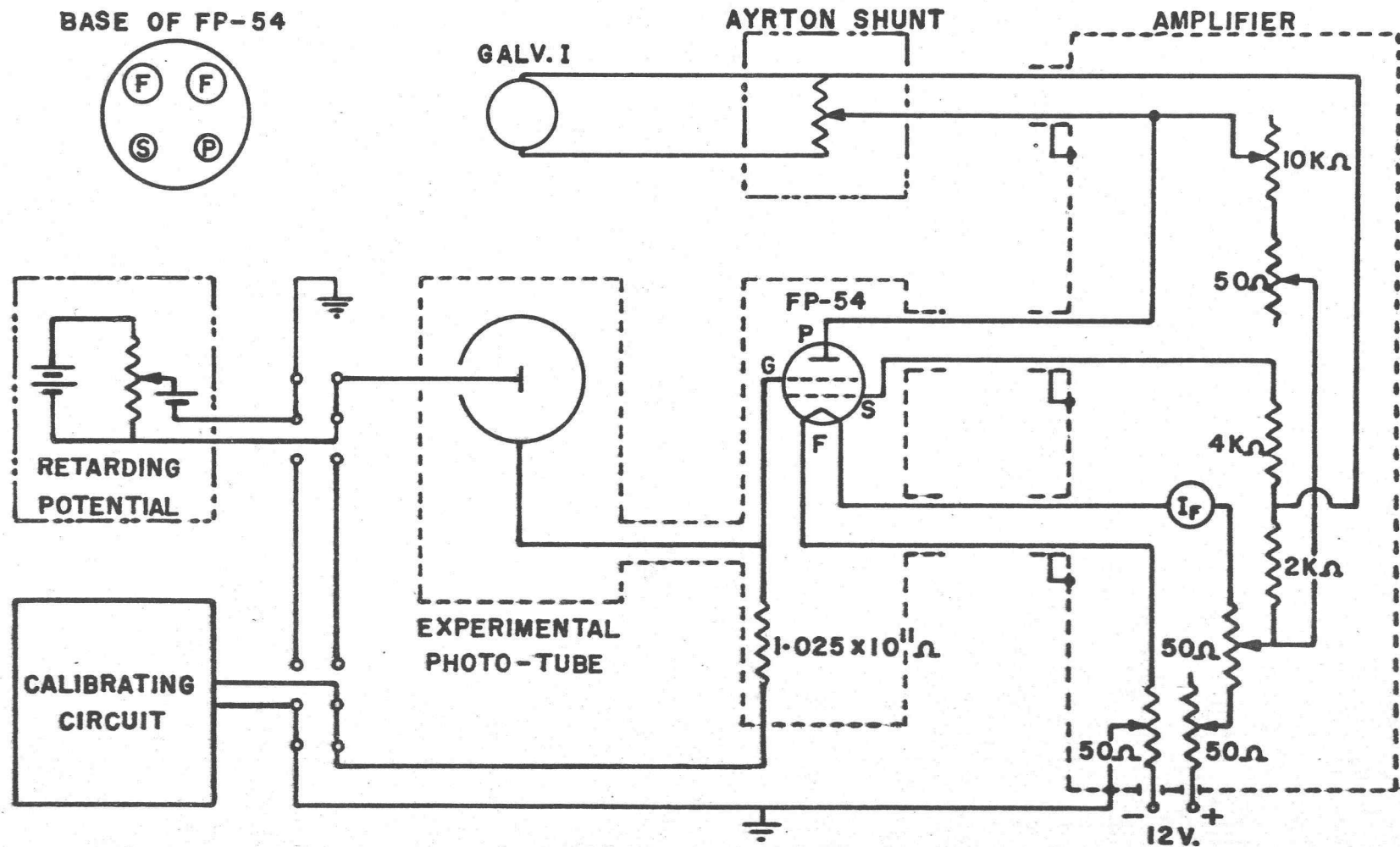50Ω

50Ω

50Ω

50Ω

12 V.

FIGURE 5. AMPLIFIER AND ASSOCIATED CIRCUITRY.

used to calibrate and balance the amplifier, also to set the retarding potential across the experimental phototube.

Galvanometers. These are mounted on a separate table to avoid vibrations. The galvanometer to scale distance is 310cm. A galvanometer lamp was made using a lens having 45mm. diameter and 19cm. focal length, the graticule is a slit 0.018 inches wide with a wire 0.0031 inches diameter mounted in the center. The image of the wire on the scale was 1-1/2mm. wide. The two galvanometers are illuminated by the same lamp, using a half silvered and a full silvered mirror. A yellow filter is included in one system to distinguish between the two images.

Apparatus Assembly and Tests. When the completed experimental phototube and vacuum system were first evacuated, the lowest pressure attained was 8.5×10^{-2}mm.Hg. The air inlet stopcock was found to be leaking, it was removed, cleaned and regreased, and a pressure of 1×10^{-2}mm.Hg. was attained. After three days with the diffusion pump on, the pressure was 4×10^{-6}mm.Hg. During this time the oven was constructed and when completed the experimental phototube and oil vapour trap was baked out. The maximum temperature obtainable was 370°C, but the tube was unevenly heated. An extra heater and a circulating fan were added to the oven. After a second bakeout lasting nine hours, with the tube at 340°C for two hours,

the tube pressure was 4×10^{-8}mm.Hg. An additional heater
was added to the oven and the tube baked out again for
twelve hours with the tube at approximately 390°C for three
hours. Tube pressure was 3×10^{-8}mm.Hg., since this was
slightly less than the vapour pressure of the diffusion
pump oil it was considered to be satisfactory.

After the tube was baked out it was discovered that
the ultra-violet light transmission through it was too low
to enable the thermocouple detector to be used and the
electron multiplier phototube detector was obtained instead.

When the apparatus was ready a study was made to
decide what light wavelength should be used. Since the
ultra-violet detector was very sensitive it was decided to
go to the lower wavelengths to increase the photocurrent
from the experimental phototube. With reference to Figure
4 it is seen that the 2483A line is approximately three
times more intense than the next intense line, 2400A.
Although the photocurrent from the silver film would
increase with lower wavelength, the lower intensity of the
2400A did not justify using it. Also the spectral range
of the detector envelope cuts off sharply at 2200A, thus
using a wavelength of 2483A instead of 2400A ensured a
greater safety margin between the operating point and the
cut-off point. For the above reasons it was decided to
use the 2483A line.

The slit width of the monochromator determines the
spectral range and intensity of the line; the intensity is
linear with slit width. With the experimental tube in
place and slit width of 0.1mm., the detector sensitivity
was approximately 900cm. of galvanometer deflection. Since
it was intended to go to a film thickness of about 400A,
which has 10% transmission, this slit width gave sufficient
sensitivity. The spectral range of the line at 0.1mm. slit
width was 6.6A which was sufficiently monochromatic for
this investigation.

The sensitivity of an electron multiplier tube is
dependent on its immediate and previous history. Thus the
sensitivity to a given light intensity is less when the
detector has just been exposed to a more intense light than
if it has just been used with a less intense light. Since
transmission through the experimental phototube was only of
the order of 3%, with no silver film, this meant measuring
light intensities which varied by a factor of 30 when
determining per cent transmission. To avoid the problem
of changing sensitivity, a light stop was inserted in the
optical system when the light intensity was measured with-
out the experimental phototube. Several light stops were
tried including closing the iris diaphragm to its smallest
diameter, also mounting a fixed aperture in the system,
but neither method was very reproducible. A quartz disc

with ground surfaces, acting like a diffuser, gave results which were reproducible within 0.5%. The disc was mounted on the mercury arc lamp housing.

The light intensity without the experimental tube or diffuser was 31,200 cm. of galvanometer deflection. With the diffuser it was about 2,500 cm. and was reproducible to about 1%, this value includes the errors due to pivoting the monochromator clear of the experimental tube. The light intensities through the experimental tube were reproducible to about 2%. The light transmission through the tube with no silver film was 46.6% of that without the tube and with the diffuser.

PROCEDURE

In order to determine the thickness of the silver film, under investigation, a separate experiment was carried out to determine the per cent light transmission through a film of known thickness. The procedure consisted of depositing a known amount of metal on a quartz disc at a given distance, determining the film thickness by the inverse square law and measuring the light transmission with the above mentioned equipment. The silver was evaporated at a pressure of 5×10^{-6}mm.Hg. in the evaporator located in the electron microscope room. The quartz discs were cleaned in hot water and detergent after each run to remove the previous film, the silver was only deposited on one half of the disc, the back of the disc was also protected. The transmission through the film was measured using the thermocouple detector and a wavelength of 2652A. Five films were deposited at each run with a total of seven runs. Typical data from one run is shown in Table 1 and the complete results are plotted in Figure 6.

The main investigation consisted of depositing a layer of silver, on the center quartz disc mounted in the experimental phototube, measuring the percentage of transmitted light through the film, and then measuring the photocurrent as a function of:

TABLE 1

Data relating ultra-violet transmission with film thickness

Weight of silver evaporated $= 0.0121$ grams

Volume of silver evaporated $= \dfrac{0.0121 \text{ grams}}{10.5 \text{ grams/c.c.}}$

Thickness of silver film at radius R cm. $= \dfrac{0.0121 \times 10^8 \text{A}}{10.5 \times 4\pi \text{ R}^2}$

| Distance from disc to source	U.V.intensity through disc with no film	Average	U.V.intensity through disc with film	Average	Transmission	Film thickness
7 cm.	17.45 17.48 17.55	17.49	5.08 5.12 5.03	5.08	29.1%	180A
10 cm.	17.0 17.2 17.1	17.1	8.97 8.95 8.92	8.95	52.3%	88A
13 cm.	17.12 17.05 17.13	17.1	10.90 10.83 10.87	10.87	63.5%	52A
15 cm.	17.58 17.55 17.65	17.59	11.83 11.68 11.67	11.73	66.8%	39A
18 cm.	17.08 17.13 17.07	17.09	12.58 12.50 12.53	12.54	73.4%	26A
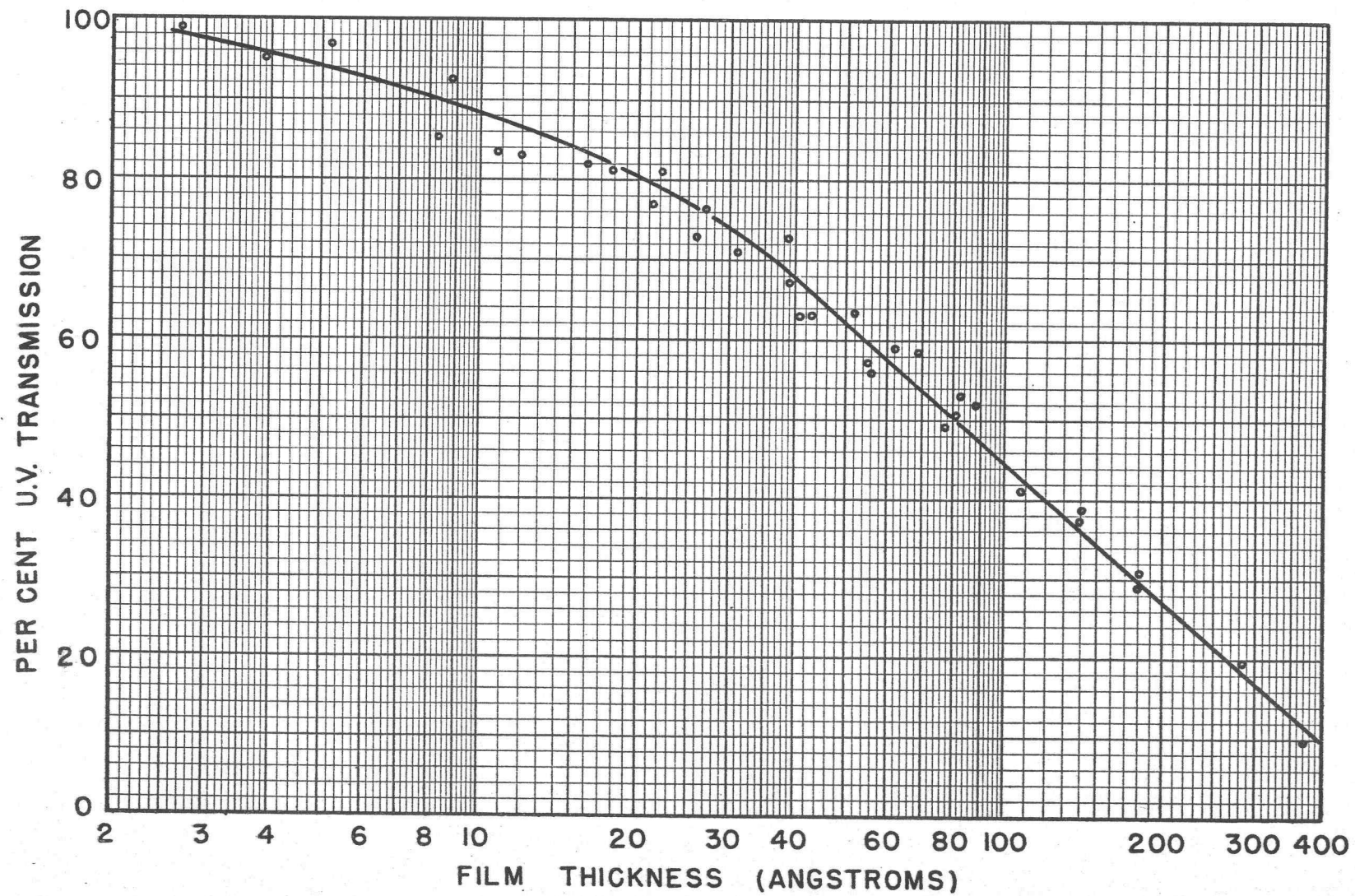
FIGURE 6.   U.V. TRANSMISSION – Vs – FILM THICKNESS

36

1. Light intensity at the light emergent side
   of the silver film.

2. Retarding potential across the phototube.

Prior to each run the amplifier sensitivity was
checked by applying a known voltage from the calibrating
circuit to the input resistance. The amplifier was used
as a null balancing device and any change in sensitivity
was relatively unimportant, however, the sensitivity
check confirmed the amplifier was functioning correctly,
and also indicated that the experimental tube had not
shorted.

When the silver was evaporated, the power to the
filaments was increased slowly to outgas the filaments and
silver. A typical evaporation schedule is shown below;
the voltage refers to the input voltage of the filament
transformer:

Voltage	Time voltage applied	Max. tube pressure
40V	30 seconds	1×10^{-6} mm.Hg.
50V	30 seconds	2×10^{-6} mm.Hg.
60V	15 seconds	2×10^{-6} mm.Hg.
70V	15 seconds	2×10^{-6} mm.Hg.
80V	45 seconds	2×10^{-6} mm.Hg.

The voltage was left on 80V for a longer period of time
when a thicker film deposit was required. After each
film was deposited the transmission through it was

measured to determine its thickness.

The photocurrent versus ultra-violet light intensity data was obtained with a 1 volt accelerating voltage across the experimental tube. The light intensity was varied, by changing the iris diaphragm aperture, and the corresponding photocurrent from the silver film was measured. The photocurrent was recorded as the voltage necessary to rebalance the amplifier. The ultra-violet light was blanked off before each measurement to check the amplifier zero. A typical set of data is tabulated in Table 2 and plotted in Figure 7; this data is for film No.5 which had 73.5% transmission and a thickness of 32A.

The photocurrent versus retarding potential data was obtained with a fixed iris diaphragm setting for each film. The procedure was to set the retarding potential, using the calibrating circuit as a reference, then measure the corresponding photocurrent. A typical set of data is tabulated in Table 3 and plotted in Figure 8; this data is also for film No.5.

The power supply for the electron multiplier photo-tube burnt out after the data for a film thickness of 255A had been obtained; since no spare components were immediately available, this concluded the investigation.

TABLE 2

Typical set of data of "photocurrent-vs-U.V.intensity"

U.V. intensity (Galv.II defl.)	Photocurrent Volts	$\times 10^{13}$ Amps.
870 cm.	0.1056	10.30
760	0.0959	9.36
660	0.0850	8.29
550	0.0698	6.81
470	0.0613	5.98
360	0.0475	4.63
234	0.0323	3.15
142	0.0211	2.06
65	0.0111	1.08
22	0.0045	0.44
845	0.1018	9.93

TABLE 3

Typical set of data of "photocurrent-vs-retarding potential"

U.V.intensity (Galv.II defl.)	Photocurrent Volts	x 10^13 Amps.	Retarding Potential
413 cm.	0.0538	5.25	+1.00v
413	0.0538	5.25	+0.30v
415	0.0536	5.23	+0.20v
417	0.0535	5.23	+0.10v
419	0.0507	4.95	0v
419	0.0478	4.66	−0.10v
418	0.0432	4.21	−0.208v
420	0.0395	3.85	−0.302v
422	0.0341	3.33	−0.402v
421	0.0279	2.72	−0.502v
420	0.0218	2.13	−0.602v
425	0.0142	1.39	−0.718v
426	0.0092	0.89	−0.804v
429	0.0041	0.40	−0.907v
429	0.0024	0.23	−0.952v
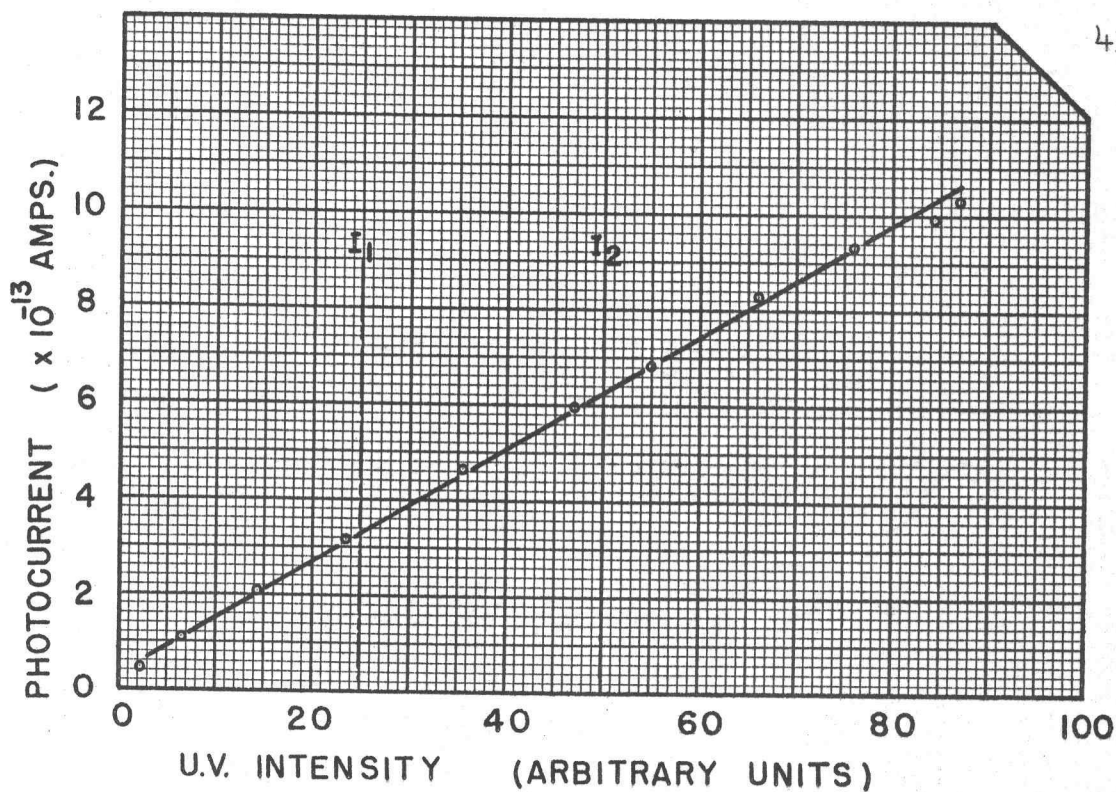
FIGURE 7.   PHOTOCURRENT – Vs – U.V. INTENSITY
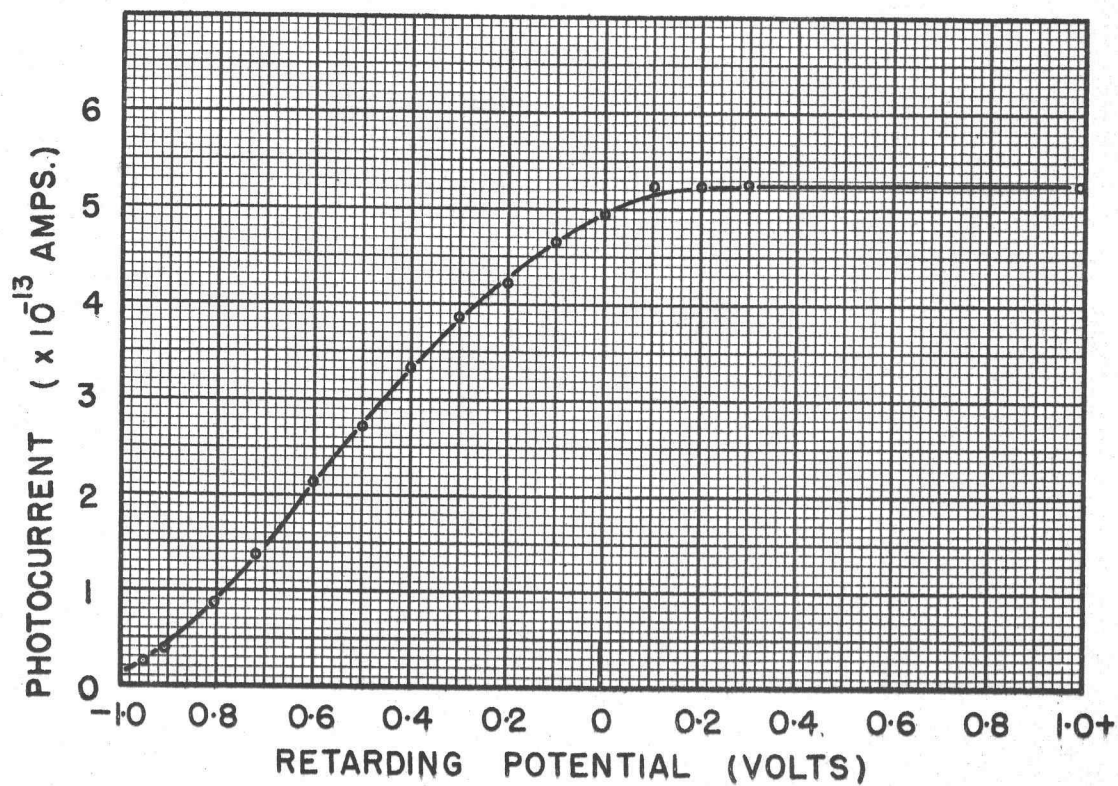
FIGURE 8.   PHOTOCURRENT – Vs – RETARDING POTENTIAL

RESULTS

As previously stated this is a study of the magnitude and the energy distribution of the photoelectric current as a function of film thickness.

Analysis of Magnitude. The magnitude of the photocurrent is plotted as a function of film thickness for different ultra-violet light intensities on Figure 9. This graph was obtained from a series of curves similar to Figure 7, but for different film thicknesses. It will be observed in Figure 9 that there is a distinct "bend" in the magnitude of the photocurrent at a film thickness of 35-40A. A similar "bend" occurs in the transmission at the same film thickness, Figure 6, but it should be pointed out that the similarity is to be expected since the two graphs are related. This critical or threshold thickness is believed to be related to the mean free path of electrons in the metal and has been studied by other experimenters in the field of resistivity of thin metal films (8, p. 232-246). A plot of resistivity versus film thickness shows that the resistivity decreases very rapidly to a constant value at a certain thickness, see Figure 10. Ells and Scott (6) found that for rapidly evaporated silver films (2 seconds) the critical thickness was 120A, whereas Oppenheim and Jaffe (11) reported the critical
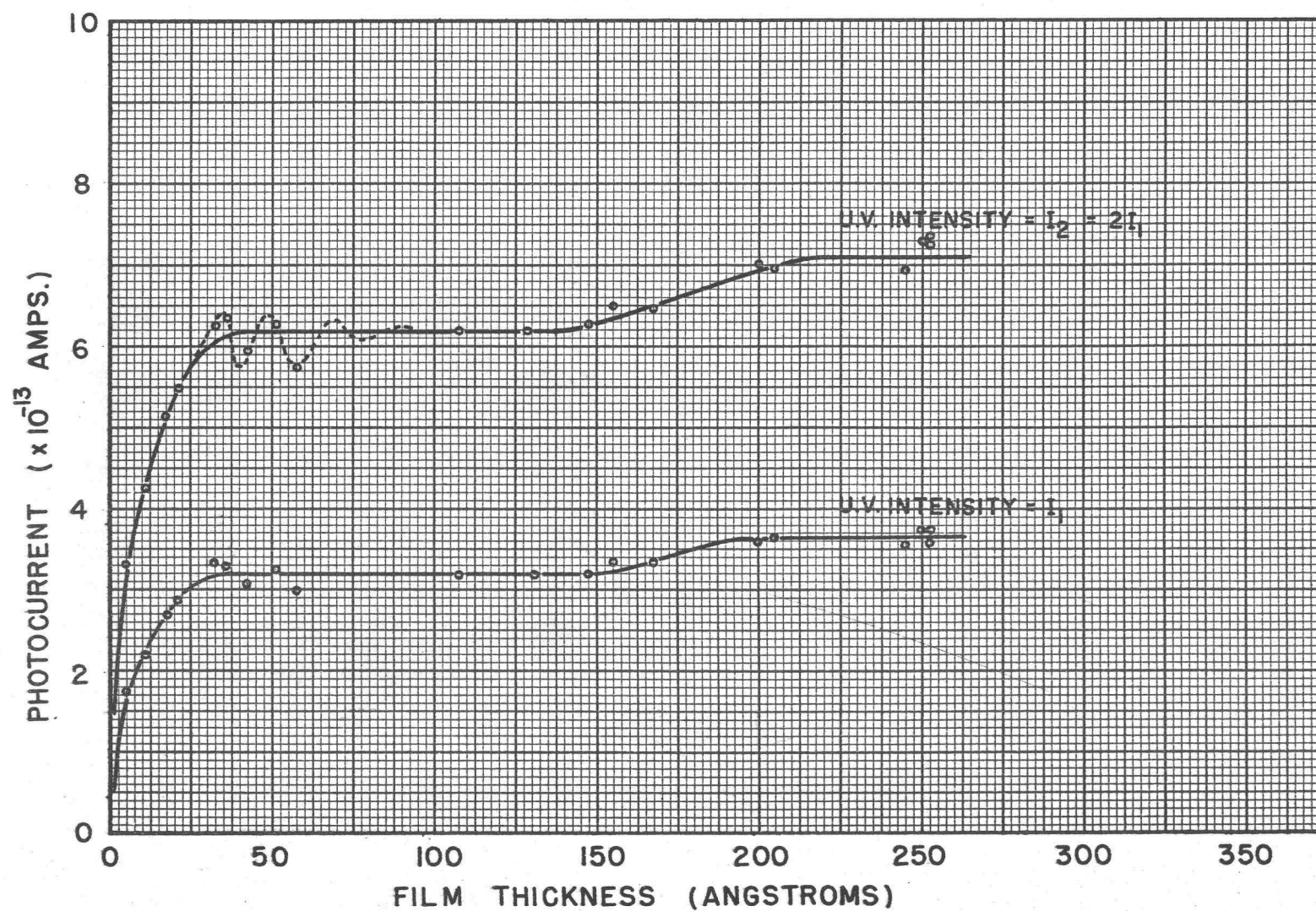
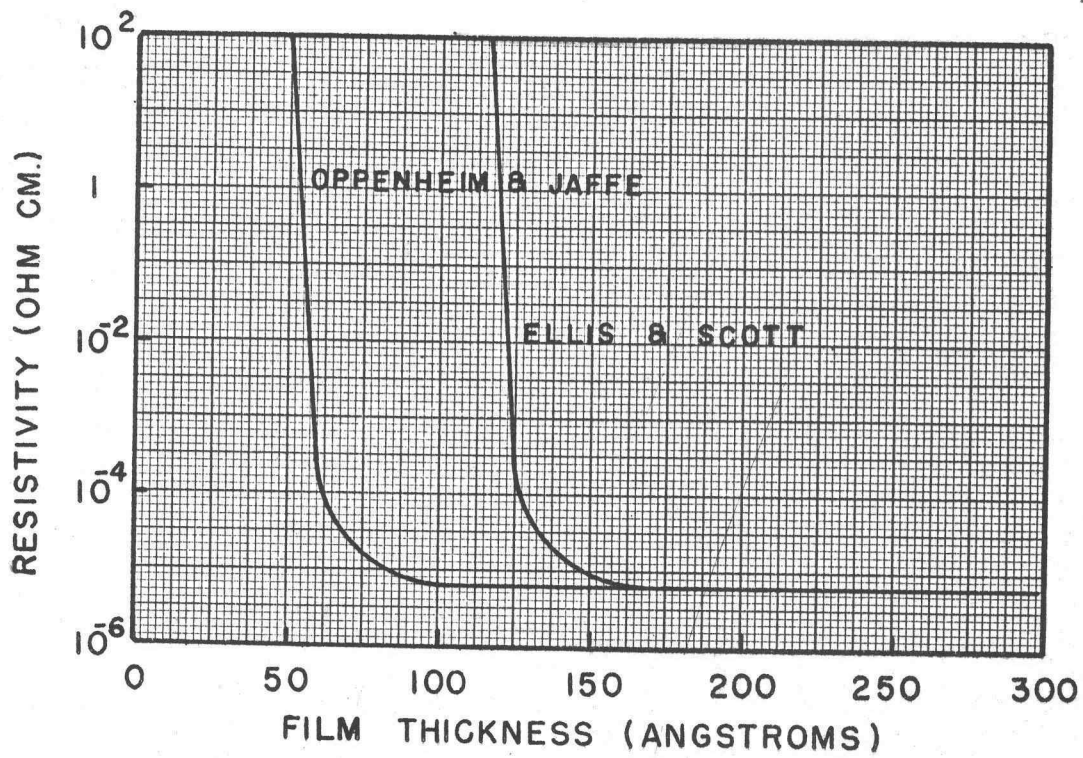FIGURE 9. PHOTOCURRENT - Vs - FILM THICKNESS FOR CONSTANT U.V. INTENSITY

43

FIGURE 10. RESISTIVITY OF SILVER FILMS

FILM THICKNESS
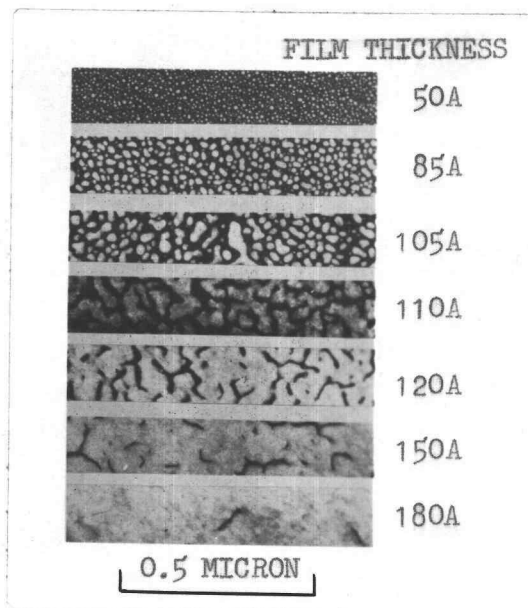50A
85A
105A
110A
120A
150A
180A

0.5 MICRON

FIGURE 11. ELECTRON MICROGRAPHS OF
THIN SILVER FILMS

thickness to be 60A. The values obtained from the photo-electric and resistivity investigations are in good experimental agreement.

A possible reason why the photocurrent increases with thickness up to a certain value is that evaporated films are known to be discontinuous when they are very thin. If the film was patchy for thicknesses less than 40A and continuous for greater thicknesses this might explain the critical value. Electron micrographs of thin silver films (13) show that they are discontinuous up to at least 150A for very rapidly evaporated films (2 seconds), and up to 560A for slowly evaporated films (20 minutes). It is evident that this patch effect does not explain the critical thickness but may explain the increase in photocurrent at the film thickness of 150-200A.

Analysis of 0 to 40A Region. Fowler's theory shows that the magnitude of the photocurrent depends on the number of electrons striking unit surface area per second. If one assumes for simplicity that all electrons have the same mean free path λ, only those electrons from a depth λ from the surface will be available for ejection at any given instant. Thus for any film thickness t greater than λ, the number of electrons arriving at the surface will be constant, hence the magnitude of the photocurrent will also be constant. If t is less than λ then the
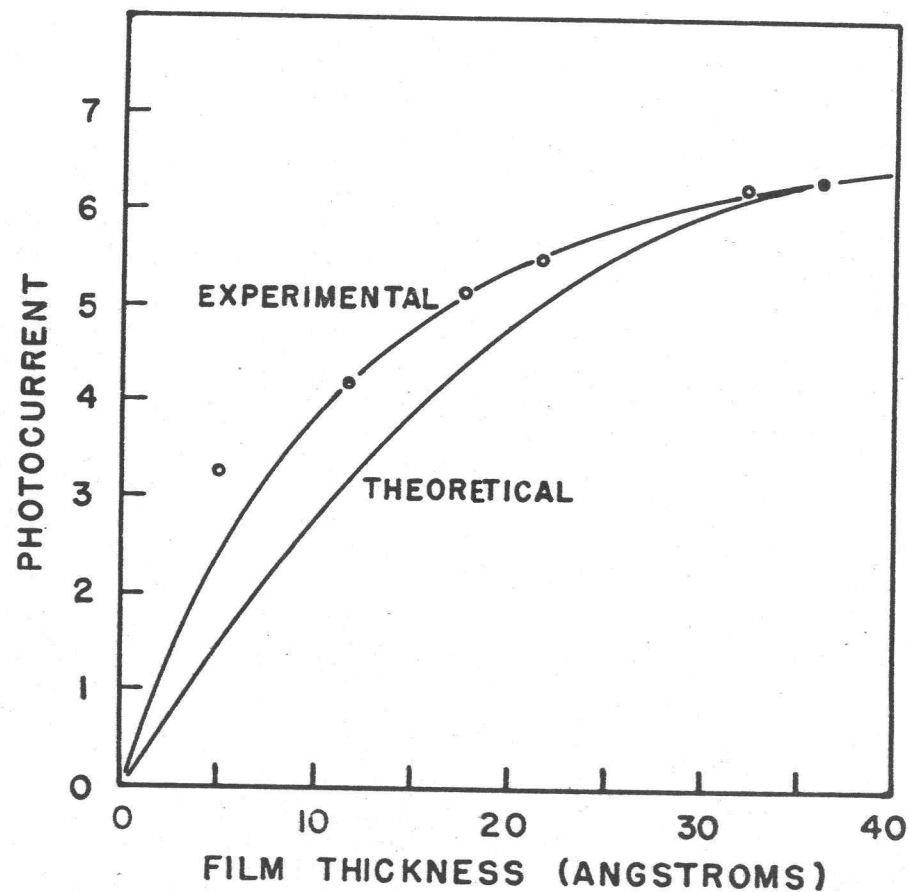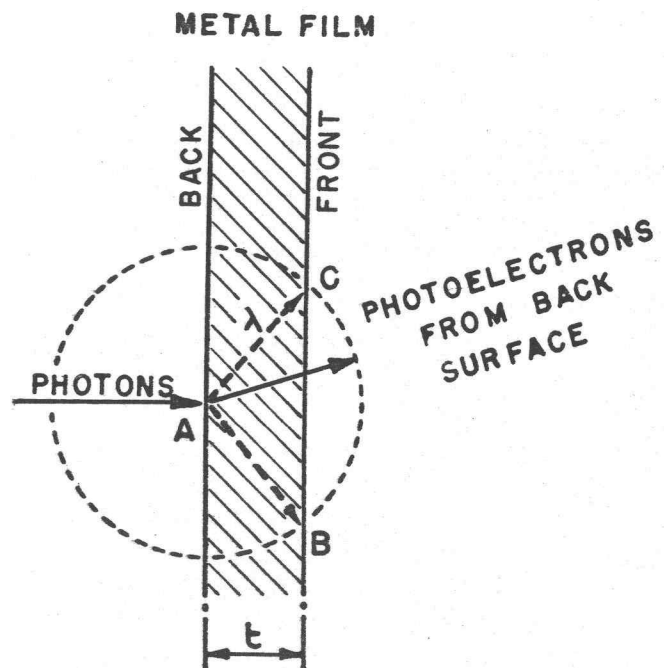
FIGURE 12.   THEORETICAL PHOTOCURRENT – Vs – FILM THICKNESS

number of electrons arriving at the surface will be
proportional to the thickness, hence the photocurrent
would be expected to be proportional to the thickness. As
can be seen from Figure 9 this is not the case, but if t
is less than λ, then electrons released from the back
surface may also be ejected through the front surface.
Consider Figure 12, the probability of an ejected electron
from the back surface leaving the front surface is the
ratio of the solid angle BAC to 2π which is $(1-t/\lambda)$; note
that only electrons traveling in the forward direction
are being considered. If the number of electrons ejected
from the front surface is Kt, where K is a constant of
proportionality, then the number of electrons that leave
the film from the back and front surfaces is $Kt(2-t/\lambda)$. A
plot of this theoretical curve and the experimental curve
for light intensity I_2 is shown on Figure 12, the agreement
between the two curves is reasonably good.

Analysis of Energy Distribution. The energy spec-
trum of the photoelectrons is obtained by differentiating
the photocurrent versus retarding potential curves,
Figure 8. This was done experimentally by measuring the
change in photocurrent for a constant change in retarding
potential. The energy spectrum of the photoelectrons for
different films is shown in Figure 13. Since the rate
of change of the photocurrent at the minimum and maximum
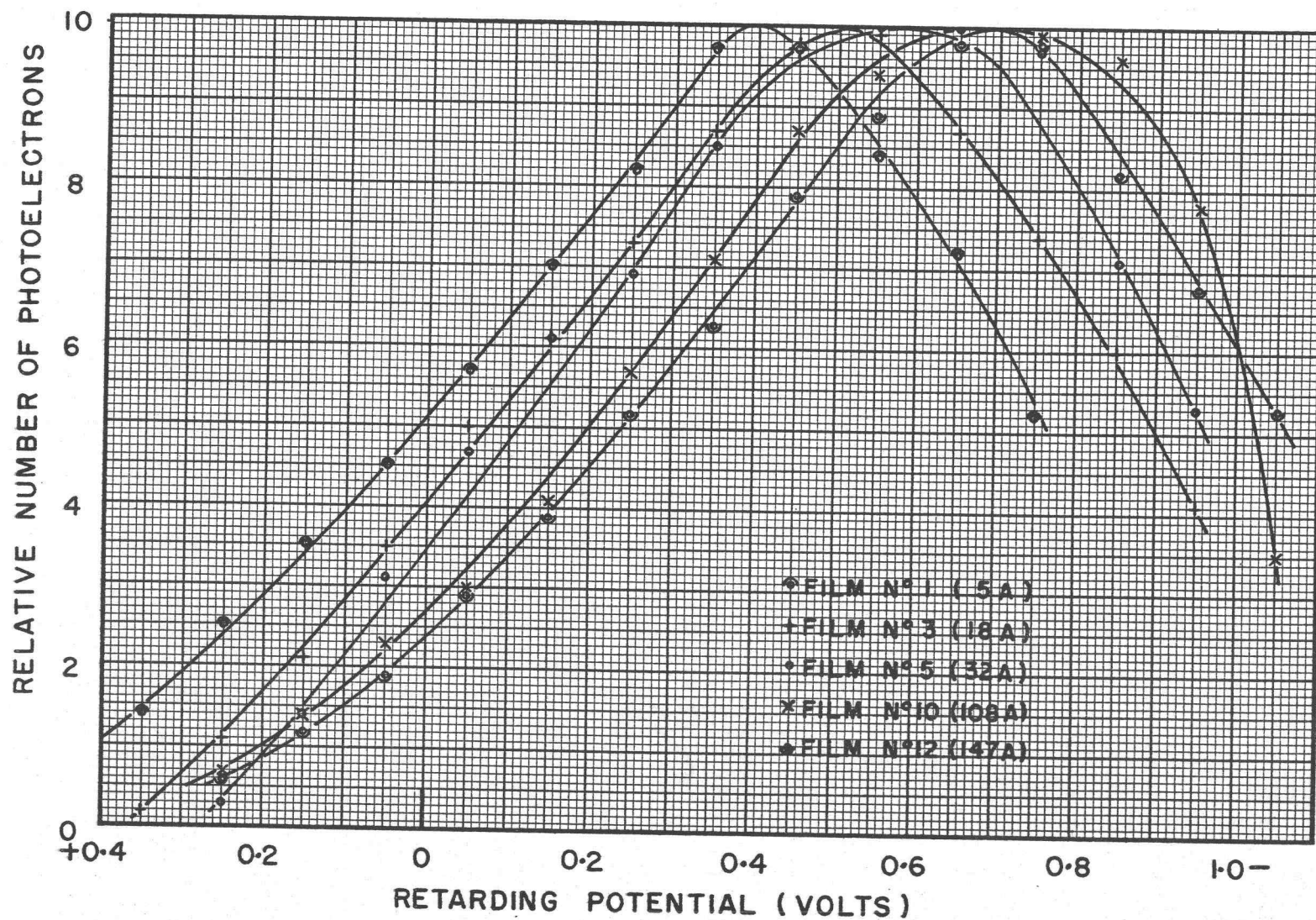
FIGURE 13. ENERGY SPECTRUM OF PHOTOELECTRONS

Legend (within figure):
- FILM N°1 (5A)
- FILM N°3 (18A)
- FILM N°5 (32A)
- FILM N°10 (108A)
- FILM N°12 (147A)

Y-axis: RELATIVE NUMBER OF PHOTOELECTRONS
X-axis: RETARDING POTENTIAL (VOLTS)

retarding potentials is of the order of the accuracy of reading, then the ends of the energy curve must be expected to be in error.

The Fowler-Dubridge graphical analysis of the energy spectrum may now be used to determine the value of V_m for each film. The value of the universal function $f(x-x_o)$ is tabulated in Table 4, the experimental data from film No. 5 and the necessary calculations for a Fowler-Dubridge plot are given in Table 5. The graphical analysis is shown in Figure 14. From a series of such graphs the "apparent change" in V_m can be determined; the results are shown in Figure 15. The agreement between the experimental and theoretical curves is only good enough to determine V_m to an accuracy of 0.015 electron volts. The "apparent change" in V_m was determined by assuming that the vertical displacement B was constant for all films. Although the points do not give a smooth curve the gradual change from 0 to 40A film thickness is very significant. The term "apparent change" has been used because the change may be due to a variation in the work function of the surface, which would produce a true change in V_m, but it may also be due to a change in contact potential between the emitter and the collector.

A change in contact potential may be expected since the collector was deposited before the investigation began

<div style="display: flex;">

TABLE 4

Universal function $f(x-x_o)$

(x_o-x)	$f(x-x_o)$
32	4.983
24	4.624
16	4.331
8	3.960
4	3.631
2	3.346
0	2.851
-1	2.524
-2	2.117
-3	1.697
-4	1.264
-5	0.830
-6	0.394

TABLE 5

Calculations for a Fowler-Dubridge plot of film number 5

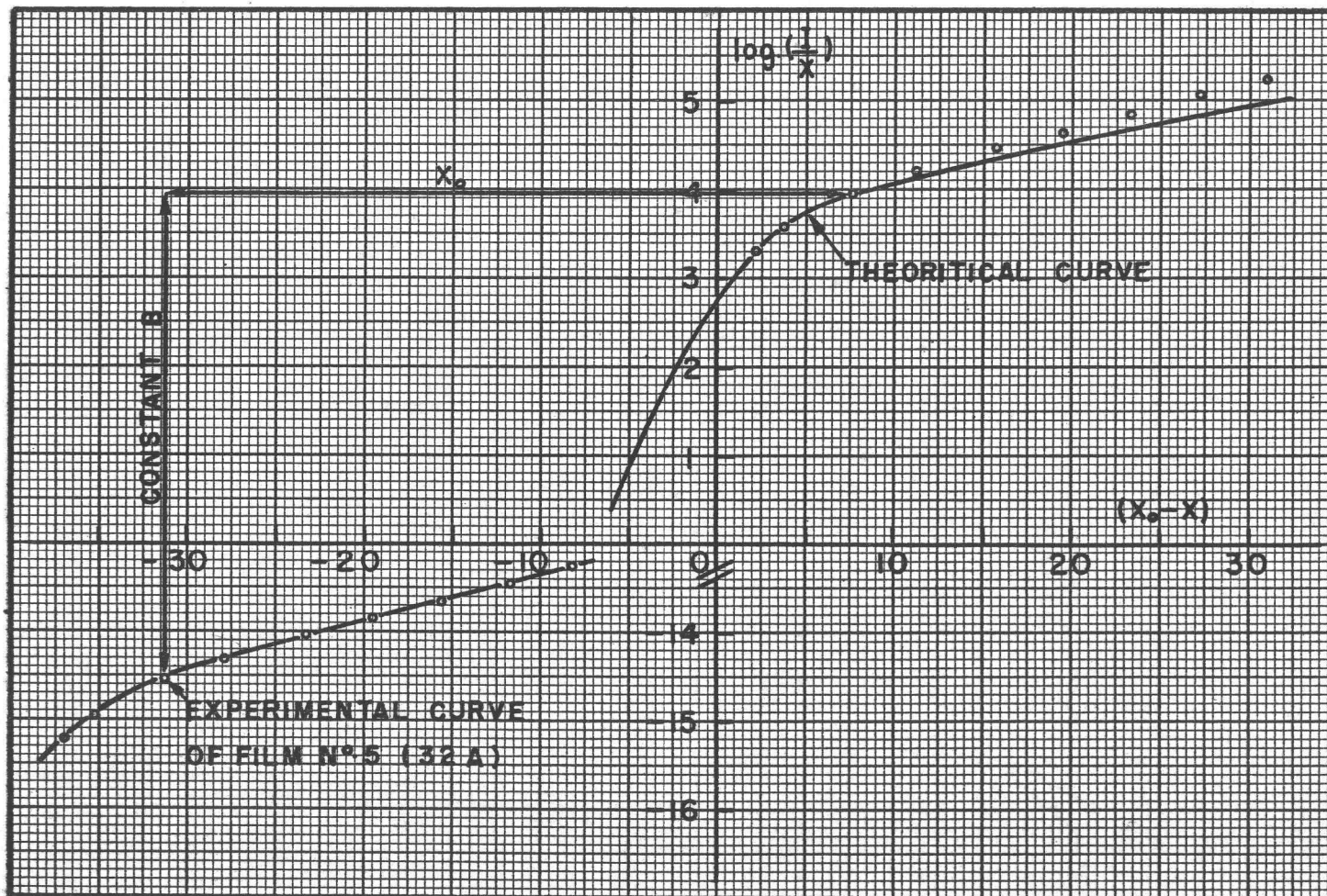| V	$x = \dfrac{Ve}{kT}$	$I \times 10^{13} A$	$(I/x) \times 10^{13}$	$\log(I/x)$
-0.208	-8.074	4.21	0.521	$\overline{14}.717$
-0.302	-11.703	3.85	0.329	$\overline{14}.517$
-0.402	-15.604	3.33	0.213	$\overline{14}.328$
-0.502	-19.486	2.72	0.140	$\overline{14}.146$
-0.602	-23.368	2.13	0.091	$\overline{15}.960$
-0.718	-27.871	1.39	0.050	$\overline{15}.698$
-0.804	-31.209	0.89	0.029	$\overline{15}.455$
-0.907	-35.207	0.40	0.011	$\overline{15}.057$
-0.952	-36.954	0.23	0.006	$\overline{16}.794$

</div>

FIGURE 14. FOWLER – DUBRIDGE ANALYSIS OF THE ENERGY SPECTRUM

and then had more metal deposited on it as the emitter was formed. If there is a difference in contact potential between emitter and collector, then the retarding potential V must be corrected accordingly and eV_m will change. Since the magnitude of the photocurrent, the per cent light transmission and the resistivity appear to change at a film thickness of the order of 40A, it is not unreasonable to assume that the work function might also vary over this range. Due to the location of the silver sources, the thickness of the "new" metal deposited on the collector would vary from 10 to 1000A when the emitter was only 40A. If it was known exactly how the work function varied with film thickness then it might be possible to determine the net effect of a film of varying thickness deposited on the collector, but it would be a coincidence if the net effect was the same as the experimental results. This leads to the suggestion that the change in V_m is due to a change in the work function of the emitter. If the work function for each film thickness is calculated from the equation $\emptyset e = h - eV_m$, see Figure 16, we see it decreases with film thickness.

Returning to the energy distribution curves on Figure 13, it is seen that the most probable electron energy increases with film thickness. If the curves are displaced by an amount approximately equal to the apparent

change in work function, then the curves are the same

general shape.　There is a slight broadening of the peaks

with increasing film thickness but this is not general

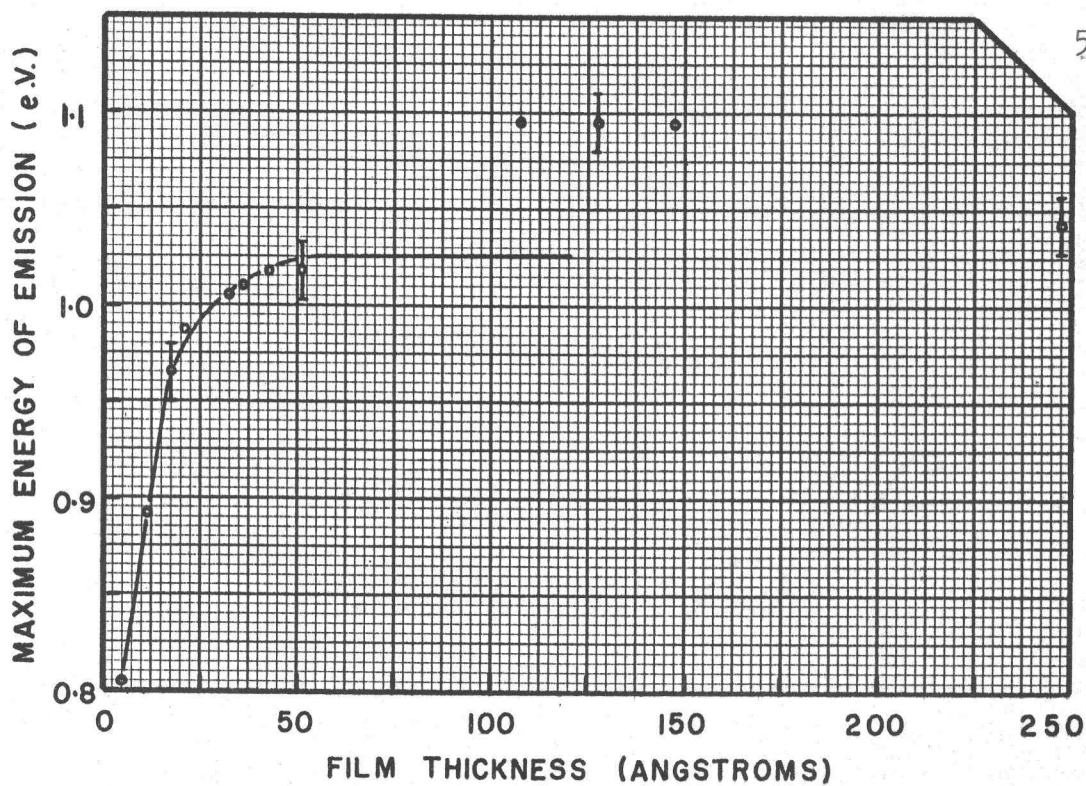since the peak for the thickness of 147A is narrower than

that for 108A.

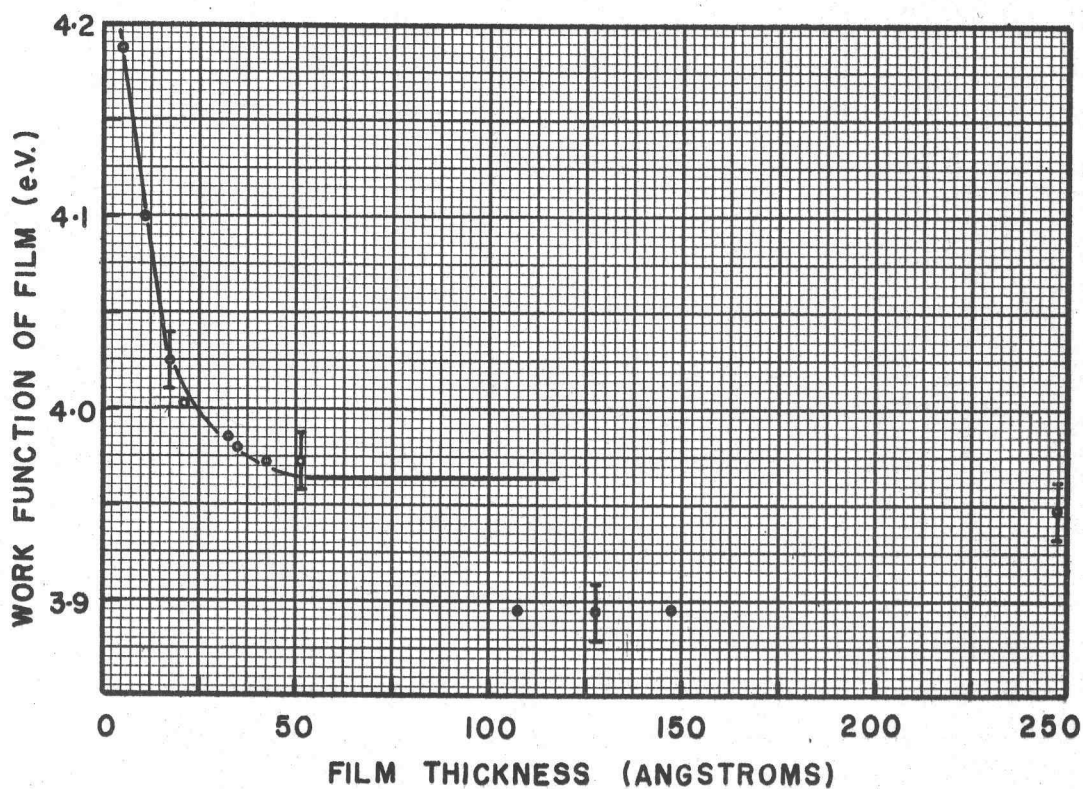FIGURE 15. MAX. ENERGY OF EMISSION – vs – FILM THICKNESS.

FIGURE 16. WORK FUNCTION – vs – FILM THICKNESS.

CONCLUSIONS

1. The results of the investigation with silver film show that there is a change in transmission of light, of wavelength 2652A, and in the magnitude of the photocurrent at a film thickness of 40A.

2. The change in magnitude of the photocurrent for film thickness of 0 to 40A has been analyzed on the assumptions that the photoelectric phenomena is a surface effect, and that the free electrons have a mean free path of 40A, within the metal. The theoretical curve is in good agreement with the experimental results.

3. The discontinuous structure of thin silver film does not appear to be responsible for the increase in photocurrent since the films are discontinuous up to at least 150A whereas the photocurrent is relatively constant after a film thickness of 40A. The structural change of the film may explain the increase in photocurrent found at a film thickness of 150-200A.

4. The energy spectrum of the photoelectrons may be analyzed on one of two assumptions:

   a. that the work function of the emitter changes

   b. that the work function of the collector changes.

4a. The change in V_m, determined by a Fowler-Dubridge plot, indicates that the work function of the

emitter decreases with increasing film thickness from
0 to 40A. If this is correct it would explain why the
photocurrent increases with film thickness.

4b. If the work function of the collector changes
and the energy spectrums are displaced by the apparent
change in V_m, as determined by the Fowler-Dubridge plot,
then the shape of the energy spectrons are approximately
the same.

BIBLIOGRAPHY

1. Alpert, Daniel. Copper isolation trap for vacuum systems. The Review of Scientific Instruments 24:1004-1005. 1953.

2. Compton, K. T. and L. W. Ross. Passage of photo-electrons through metals. Physical Review 13:374-391. 1919.

3. Dubridge, Lee Alvin. Theory of the energy distribution of photoelectrons. Physical Review 43:727-741. 1933.

4. Dubridge, Lee Alvin. New theories of the photo-electric effect. Paris, Hermann, Editeurs, 1935. 56 numb. leaves. (Actualities scientifique et industrielles. No.268).

5. Dubridge, Lee Alvin and Hart Brown. An improved d.c. amplifying circuit. The Review of Scientific Instruments 4:532-536. 1936.

6. Ells, C. E. and G. D. Scott. The structure of sputtered silver films. Journal of Applied Physics 23:31-34. 1952.

7. Fowler, R. H. The analysis of photoelectric sensitivity curves for clean metals at various temperatures. Physical Review 38:45-56. 1931.

8. Holland, L. Vacuum deposition of thin films. New York, John Wiley and Sons, 1956. 541p.

9. Hughes, Arthur L. and Lee Alvin Dubridge. Photoelectric phenomena. New York, McGraw-Hill, 1932. 531 numb. leaves.

10. Leeds and Northrup Company. Students potentiometer and accessories. Catalog E-50B(1). Leeds and Northrup Company, 1953. 15p.

11. Oppenheim, Uri and Joseph H. Jaffe. Resistivity of thin silver films. Journal of Applied Physics 24: 1521. 1953.

12.   Perry, Richard Lee. Measurements of changes of
          photoelectric probability factor due to surface
          contamination of aluminum. Master's thesis.
          Corvallis, Oregon State College, 1955. 38 numb.
          leaves.

13.   Sennett, R. S. and G. D. Scott. The structure of
          evaporated metal films and their optical prop-
          erties. Journal of the Optical Society of
          America 40:203-211. 1950.

14.   Stuhlmann, Otto Jr. The variation of the photoelec-
          tric current with thickness of metal. Physical
          Review 20:65-74. 1922.

APPENDIX

LIST OF EQUIPMENT

Cenco Megavac mechanical pump.

Eimac HV-1 oil diffusion pump.

Veeco RG75 non-burnout ionization gauge:

Filament voltage	3 to 5V.
Filament current	4 to 6 amps.
Grid	+150V.
Grid current	10 mA.
Collector	-20 to -50V.
Sensitivity	100μA/micron Hg. pressure at 10mA grid current.
Grid outgas	6.3 to 7.5V at 10 amps.

Radiation Laboratory ionization gauge power supply.

R.C.A. type WV-84A direct current microammeter.

Bausch and Lomb Grating Monochromator (250cm. focal length)

Mercury arc lamp with power supply.

Sola 115V. 250V.A. constant voltage transformer.

R.C.A. IP28 phototube and power supply.

Variac and 2.5V 10A. transformer for evaporating silver.

FP-54 Electrometer tube and housing:

Input resistance	10^{16} Ω.
Control grid current	10^{-15} A.
Filament current	90 mA.
Screen current	500 mA.
Filament voltage	2.5V.
Plate voltage	6.0V.
Space charge grid	4.0V.
Plate current	60 μA.
Mutual conductance	20 μA/V.
Plate resistance	45,000 Ω.

Brown and Dubridge amplifier.

12V. Storage battery and battery charger.

Two Ayrton Shunts.

Two Leeds and Northrup Galvanometers, Model No.2284 type HS.
Sensitivity   0.192 μV/mm. deflection at 1 meter.

Galvanometer lamp and scale.

Calibrating circuit, see reference 10.